Decay of the pair correlations and small-angle scattering for binary liquids and glasses

2006 J. Phys.: Condens. Matter 18 11443

(http://iopscience.iop.org/0953-8984/18/50/004)

INSTITUTE OF PHYSICS PUBLISHING JOURNAL OF PHYSICS: CONDENSED MATTER

J. Phys.: Condens. Matter **18** (2006) 11443–11469 doi:10.1088/0953-8984/18/50/004

Decay of the pair correlations and small-angle scattering for binary liquids and glasses

Philip S Salmon

Department of Physics, University of Bath, Bath BA2 7AY, UK

Received 9 September 2006, in final form 24 October 2006
Published 27 November 2006
Online at stacks.iop.org/JPhysCM/18/11443

Abstract

The origin of extended-range ordering in binary liquids and glasses is investigated. The starting point is a simple model pair potential which includes both Coulomb and dispersion forces. For this model, the behaviour of the Bhatia–Thornton partial structure factors at small scattering vector values is examined and also the asymptotic behaviour of the associated partial pair correlation functions in real space. The results are compared with the observed real space pair correlation functions for a range of liquid and glassy systems for which accurate partial structure factors have been measured by using neutron diffraction. It is found that the extended range ordering can often be accounted for by using an exponentially damped oscillatory function with a wavelength of oscillation given by $\approx 2\pi/k_{\rm PP}$, where $k_{\rm PP}$ is the position of the principal peak in the measured partial structure factors. Sometimes this exponentially damped oscillatory function also accounts for the observed behaviour of the real space data at relatively small distances as in the case of the concentration–concentration pair correlation function for molten Ag_2Se and for glassy $GeSe_2$, $ZnCl_2$ and GeO_2. For these glasses, all of the Bhatia–Thornton pair correlation functions in real space eventually decay with a common wavelength of oscillation and a common decay length. The limitations associated with the use of simple model pair potentials to analyse the experimental data sets are discussed. In addition, the effect on the small-angle scattering and asymptotic decay of the real space pair correlation functions of including a term corresponding to ion-induced dipole interactions in the pair potential is briefly considered. An analytical expression is also given for the real space manifestation of the Lorch modification function.

(Some figures in this article are in colour only in the electronic version)

1. Introduction

The atomic structure of liquids and glasses at distances greater than the nearest-neighbour remains an outstanding challenge in the science of disordered materials [1–8]. For network

forming materials, the focus of attention is usually on the origin of a so-called first sharp diffraction peak (FSDP) in the measured diffraction patterns at a scattering vector $k_{\rm FSDP} \approx 1$–1.5 Å^{-1}. This feature does not, for example, appear in the diffraction patterns of simple molten salts [9] and its occurrence is taken to be a signature of intermediate-range atomic ordering having a periodicity $2\pi/k_{\rm FSDP}$ and a coherence length $2\pi/\Delta k_{\rm FSDP}$, where $\Delta k_{\rm FSDP}$ is the full width at half maximum of the FSDP. Recently, diffraction experiments on network glasses have shown that there is also atomic ordering that extends to distances well beyond the domain of the FSDP and which has a periodicity given by approximately $2\pi/k_{\rm PP}$, where $k_{\rm PP} \approx 2.0$–2.7 Å^{-1} is the position of the principal peak in the measured diffraction patterns [10–12]. It is therefore important to understand the origin of the intermediate- and extended-range ordering, especially as it should give structural insight into important phenomena such as the relative fragility of glass forming liquids [12, 13], the nucleation and growth of crystals from the liquid or glassy phase [14–16] and the existence, or otherwise, of polyamorphic phase transitions i.e. distinct changes in the structure of a liquid or glass with change of density [13, 17–20]. It is also important to develop a link between the extended range ordering and the asymptotic decay of pair correlation functions for which theories have been developed [21–25]. This asymptotic behaviour is of interest not only for bulk uniform fluids but also for inhomogeneous fluids; e.g., the eventual decay of the pair correlation functions for a simple fluid will be the same in the bulk and at large distances away from an interface such as a planar wall [21, 26]. In addition, large-scale computer simulations of liquids and glasses are becoming increasingly sensitive to the asymptotic behaviour of the pair correlation functions and, concomitantly, to the small-k behaviour of the partial structure factors, where k denotes the magnitude of the scattering vector [27, 28].

Motivation is therefore provided to examine the origin of extended-range ordering in structurally disordered systems and to search for the signature of this ordering in the measured partial pair correlation functions. A suitable starting point is provided by the Ornstein–Zernike equations for an isotropic binary system [29–31] and the formalism is developed for the so-called Bhatia–Thornton [32] number–number, $S_{\rm NN}(k)$, concentration–concentration, $S_{\rm CC}(k)$, and number–concentration, $S_{\rm NC}(k)$, partial structure factors, which separate the contributions to a measured diffraction pattern from the number density and concentration fluctuations (section 2.1). For definiteness it will be assumed that expressions describing the equilibrium properties of the liquid phase also provide a guide to the properties of the corresponding glass, i.e. to the liquid phase after it has fallen out of equilibrium [33]. The development of the formalism follows that of Tosi and co-workers [34] and Evans and co-workers [21–23], but the previous work is extended to two-component systems of arbitrary composition and the effects of dispersion and ion-induced dipole forces are considered in greater detail. The Bhatia–Thornton partial structure factors are often used by experimentalists and the use of number density and concentration as the choice of variables enables the formalism to be readily applied to non-ionic systems, where the relation between concentration and charge density fluctuations can be non-trivial [7]. When possible, a comparison is made with previous results, e.g. those obtained for symmetrical binary mixtures.

To provide a benchmark for testing more complicated scenarios, a simple model pair potential is considered, in which there are short-ranged repulsive, Coulomb and dispersion terms (section 2.2). For this potential, the small-k behaviour of the Bhatia–Thornton $S_{IJ}(k)$ (where $I, J = {\rm N}, {\rm C}$) is examined, corresponding to the small-angle scattering measured in a diffraction experiment, and it is found that these partial structure factors are described by terms with different lowest odd integer powers of k (section 2.3), in agreement with the recent results of Kjellander and Forsberg [35]. One feature of the Bhatia–Thornton formalism is an

occasional decoupling between the number density and concentration fluctuations as illustrated in section 2.4 for symmetrical binary mixtures. In real space, the asymptotic decay of the pair correlation functions is first considered for the case of the model pair potential when dispersion forces are *absent* (section 2.5). Recourse is made to the results of Leote de Carvalho and Evans [22], who made a pole analysis of the k-space solutions to the Ornstein–Zernike equations and found that the pair correlation functions all decay either (i) with a monotonic exponential dependence having a common decay length or (ii) with an exponentially damped oscillatory dependence having a common decay length and common wavelength of oscillation. The corresponding decay of the moments of the Bhatia–Thornton pair correlation functions is also discussed (section 2.6). The asymptotic decay of the pair correlation functions is then considered for the case of the model pair potential when dispersion forces are *present*. In this case, the longest ranged behaviour in real space is instead expected to have a power law dependence [23, 35, 36] and relevant expressions are given in section 2.7.

The behaviour of the *measured* Bhatia–Thornton pair correlation functions is then considered for a variety of different binary liquid and glassy systems for which sufficiently accurate experimental results are available (section 3). For several of the systems it is found that, within the experimental error, the measured extended range ordering can be described in terms of exponentially damped oscillatory functions, i.e. it has some of the characteristics expected for the asymptotic decay of the pair correlation functions as deduced from a pole analysis of the Ornstein–Zernike equations for the model pair potential when dispersion forces are absent. The implications of the results are discussed (section 4) before conclusions are drawn (section 5).

2. Theory

2.1. Total pair correlation functions for a binary system

Consider an isotropic binary system comprising chemical species a and b. The partial pair distribution functions $g_{ij}(r)$ give a measure of the probability of finding any two particles labelled by i and j ($i, j = a, b$) separated by a distance $r_{ij} = |\mathbf{r}_i - \mathbf{r}_j|$. The total pair correlation functions are defined by $h_{ij}(r) \equiv g_{ij}(r) - 1$ and, therefore, also describe the overall correlation between particles i and j. They are related to the direct pair correlation functions $c_{ij}(r)$ via the Ornstein–Zernike equations, which, for a binary system, can be written as [29–31]

$$h_{ij}(r_{12}) = c_{ij}(r_{12}) + \rho_a \int \mathrm{d}^3 r_3 \, c_{ia}(r_{13}) h_{aj}(r_{32}) + \rho_b \int \mathrm{d}^3 r_3 \, c_{ib}(r_{13}) h_{bj}(r_{32}) \tag{1}$$

where $\rho_i \equiv N_i / V$ is the number density of particles of species i and V is the volume. Equation (1) defines $c_{ij}(r)$ and thereby separates the total correlation of atoms i and j into a direct part which depends only on their relative position r_{ij} and indirect parts which depend, through the integrands, on the correlated positions of all the other particles. This description of the structure does not depend on the equilibrium state of the system and should therefore apply to both liquids and glasses [37]. Application of the convolution theorem enables the Ornstein–Zernike equations to be written in Fourier space as

$$\hat{h}_{ij}(k) = \hat{c}_{ij}(k) + \rho_a \hat{c}_{ia}(k) \hat{h}_{aj}(k) + \rho_b \hat{c}_{ib}(k) \hat{h}_{bj}(k) \tag{2}$$

where the Fourier transform of $h_{ij}(r)$ is given by

$$\hat{h}_{ij}(k) = \frac{4\pi}{k} \int_0^\infty \mathrm{d}r \, r \, h_{ij}(r) \sin(kr) \tag{3}$$

and an equivalent expression defines $\hat{c}_{ij}(k)$ as the Fourier transform of $c_{ij}(r)$. By solving these Ornstein–Zernike equations it follows that

$$\begin{aligned}\hat{h}_{aa}(k) &= \frac{\hat{c}_{aa}(k) + \rho_{\mathrm{b}}[\hat{c}_{ab}(k)^2 - \hat{c}_{aa}(k)\hat{c}_{bb}(k)]}{D(k)} \\ \hat{h}_{bb}(k) &= \frac{\hat{c}_{bb}(k) + \rho_{\mathrm{a}}[\hat{c}_{ab}(k)^2 - \hat{c}_{aa}(k)\hat{c}_{bb}(k)]}{D(k)} \\ \hat{h}_{ab}(k) &= \frac{\hat{c}_{ab}(k)}{D(k)} = \frac{\hat{c}_{ba}(k)}{D(k)} = \hat{h}_{ba}(k)\end{aligned} \tag{4}$$

where $\hat{c}_{ab}(k) = \hat{c}_{ba}(k)$ and the common denominator

$$D(k) = \left[1 - \rho_a \hat{c}_{aa}(k)\right]\left[1 - \rho_b \hat{c}_{bb}(k)\right] - \rho_a \rho_b \hat{c}_{ab}(k)^2. \tag{5}$$

The so-called Faber–Ziman [38] partial structure factors (also see [39]) are defined by $S_{ij}(k) \equiv \rho \hat{h}_{ij}(k)$, where $\rho = \rho_a + \rho_b = N/V$ is the total atomic number density of the system and N is the total number of particles. In a diffraction experiment on a binary system, the measured coherent scattered intensity can be represented in terms of these functions by the total structure factor [40]

$$F(k) = x_a^2 f_a^2 [S_{aa}(k) - 1] + 2x_a x_b f_a f_b [S_{ab}(k) - 1] + x_b^2 f_b^2 [S_{bb}(k) - 1] \tag{6}$$

where $x_i = N_i/N$ and f_i are the atomic fraction and coherent scattering length of species i respectively. The Faber–Ziman partial structure factors are the functions most often shown in experimental work. Often it is useful, however, to re-write the measured intensity in terms of the Bhatia–Thornton [32] number–number, $S_{\mathrm{NN}}(k)$, concentration–concentration, $S_{\mathrm{CC}}(k)$, and number–concentration, $S_{\mathrm{NC}}(k)$, partial structure factors such that

$$F(k) = \langle f \rangle^2 [S_{\mathrm{NN}}(k) - 1] + x_a x_b (f_a - f_b)^2 [S_{\mathrm{CC}}(k)/x_a x_b - 1] + 2\langle f \rangle (f_a - f_b) S_{\mathrm{NC}}(k) \tag{7}$$

where $\langle f \rangle = x_a f_a + x_b f_b$ is the average coherent scattering length (also see [29]). $S_{\mathrm{NN}}(k)$ will therefore be measured directly in a diffraction experiment if $f_a = f_b$, whereas $S_{\mathrm{CC}}(k)$ will be measured directly if $\langle f \rangle = 0$. Since the Bhatia–Thornton $S_{IJ}(k)$ (where $I, J = \mathrm{N}, \mathrm{C}$) separate the number density from the concentration fluctuations they have a simple interpretation in the thermodynamic ($k = 0$) limit, where [32]

$$S_{\mathrm{NN}}(0) = \rho k_{\mathrm{B}} T \chi_T + \delta^2 S_{\mathrm{CC}}(0) \tag{8}$$

$$S_{\mathrm{CC}}(0) = k_{\mathrm{B}} T / (\partial^2 G / \partial x_a^2)_{T,p,N} \tag{9}$$

$$S_{\mathrm{NC}}(0) = -\delta S_{\mathrm{CC}}(0). \tag{10}$$

In these equations k_{B} is the Boltzmann constant, T is the absolute temperature, p is the pressure, G is the Gibbs free energy per particle, χ_T is the isothermal compressibility, $\delta \equiv \rho(v_a - v_b)$ is the dilation factor, and v_i is the partial molar volume per particle of chemical species i. We note that in a neutron or x-ray diffraction experiment, a complete diffraction pattern is made by averaging the 'snapshots' taken of the system by each of the incident quanta, i.e. it is made by summing up all the contributions that arise from the scattered intensity from all the coherence volumes in the sample [40]. Since the number density and concentration of particles within the different coherence volumes is not fixed, the diffraction experiments are sensitive to fluctuations in these quantities.

The number–number partial structure factor is related to the corresponding partial pair distribution function by the Fourier transform

$$S_{\mathrm{NN}}(k) - 1 = \frac{4\pi\rho}{k} \int_0^\infty \mathrm{d}r\, r [g_{\mathrm{NN}}(r) - 1] \sin(kr) \tag{11}$$

and equivalent Fourier transforms relate $[S_{CC}(k)/x_a x_b - 1]$ to $g_{CC}(r)$ and $S_{NC}(k)/x_a x_b$ to $g_{NC}(r)$. In terms of the total pair correlation functions for the atomic species

$$\begin{aligned} h_{NN}(r) &\equiv g_{NN}(r) - 1 = x_a^2 h_{aa}(r) + x_b^2 h_{bb}(r) + 2x_a x_b h_{ab}(r) \\ h_{CC}(r) &\equiv g_{CC}(r) = x_a x_b [h_{aa}(r) + h_{bb}(r) - 2h_{ab}(r)] \\ h_{NC}(r) &\equiv g_{NC}(r) = x_a[h_{aa}(r) - h_{ab}(r)] - x_b[h_{bb}(r) - h_{ab}(r)]. \end{aligned} \tag{12}$$

The topological ordering in the system is described by $g_{NN}(r)$, which gives the sites of the scattering nuclei but does not distinguish between the chemical species that decorate those sites; the chemical ordering is described by $g_{CC}(r)$, which has positive or negative peaks when there is a preference for like or unlike neighbours respectively; and the correlation between sites and their occupancy by a given chemical species is described by $g_{NC}(r)$ [9, 41]. By using equations (4) it can then be shown that the Bhatia–Thornton partial structure factors are related to the Fourier transforms of these total pair correlation functions by

$$S_{NN}(k) = \rho \hat{h}_{NN}(k) + 1 = \frac{1 - \rho \hat{c}_{CC}(k)}{D(k)} \tag{13}$$

$$\frac{S_{CC}(k)}{x_a x_b} = \rho \hat{h}_{CC}(k) + 1 = \frac{1 - \rho \hat{c}_{NN}(k)}{D(k)} \tag{14}$$

$$\frac{S_{NC}(k)}{x_a x_b} = \rho \hat{h}_{NC}(k) = \frac{\rho \hat{c}_{NC}(k)}{D(k)} \tag{15}$$

where equation (5) can be re-written as

$$D(k) = [1 - \rho \hat{c}_{NN}(k)][1 - \rho \hat{c}_{CC}(k)] - \rho_a \rho_b \hat{c}_{NC}(k)^2 \tag{16}$$

and the direct pair correlation functions $c_{NN}(r)$, $c_{CC}(r)$ and $c_{NC}(r)$ are defined in terms of the $c_{ij}(r)$ for the atomic species by expressions that are equivalent to equations (12).

2.2. Binary system with both Coulomb and dispersion forces

Consider a binary ionic system where chemical species a and b have positive and negative charges of $Z_a e$ and $Z_b e$ respectively and e is the elementary charge. Let the interaction between any two particles labelled by i and j separated by a distance r be represented by a pair potential which contains a short-ranged repulsive term $\phi_{ij}^{sr}(r)$, a Coulomb term $\phi_{ij}^{Coul}(r) \propto r^{-1}$, and a dispersion term $\phi_{ij}^{disp}(r) \propto r^{-6}$ such that

$$\phi_{ij}(r) = \phi_{ij}^{sr}(r) + \frac{Z_i Z_j e^2}{\epsilon r} - \frac{A_{ij}}{r^6} \tag{17}$$

where $\epsilon \equiv 4\pi \varepsilon_r \varepsilon_0$, ε_r is the dimensionless relative dielectric constant of the medium in which the ions are immersed and ε_0 is the vacuum permittivity. The dispersion term results from induced dipole—induced dipole interactions and A_{ij} is a parameter ($\geqslant 0$) which depends on the polarizability of the ions [42]. Equation (17) is an example of a rigid-ion potential and represents one of the simplest simulation models for ionic systems [43–45]. If it is assumed that at large r the direct correlation function is given by $c_{ij}(r) = -\beta \phi_{ij}(r)$ [30], where $\beta \equiv 1/k_B T$, then

$$c_{ij}(r) \equiv c_{ij}^{sr}(r) - \beta \frac{Z_i Z_j e^2}{\epsilon r} + \beta \frac{A_{ij}}{r^6}. \tag{18}$$

The Fourier transform of $c_{ij}(r)$ is then given by

$$\hat{c}_{ij}(k) = \hat{c}_{ij}^{sr}(k) - \frac{4\pi \beta Z_i Z_j e^2}{\epsilon k^2} + \alpha_{ij} k^3 \tag{19}$$

where $\alpha_{ij} = \pi^2\beta\, A_{ij}/12$ [23, 36]. The $c_{ij}^{\rm sr}(r)$ will be taken to be exponentially short ranged such that at small k

$$\hat{c}_{ij}^{\rm sr}(k) = c_{ij}^{{\rm sr}(0)} + c_{ij}^{{\rm sr}(2)}k^2 + c_{ij}^{{\rm sr}(4)}k^4 + \cdots \tag{20}$$

where the moments are given by

$$c_{ij}^{{\rm sr}(2n)} = \frac{4\pi(-1)^n}{(2n+1)!}\int_0^\infty {\rm d}r\, c_{ij}^{\rm sr}(r)\, r^{2n+2} \tag{21}$$

and $n = 0, 1, 2, \ldots$.

By using equation (19) and the condition for overall charge neutrality $x_a Z_a + x_b Z_b = 0$ it can be shown that the Fourier transforms of the direct correlation functions $c_{\rm NN}(r)$, $c_{\rm CC}(r)$ and $c_{\rm NC}(r)$ are given by

$$\hat{c}_{\rm NN}(k) = \hat{c}_{\rm NN}^{\rm sr}(k) + \alpha_{\rm NN}\, k^3 \tag{22}$$

$$\hat{c}_{\rm CC}(k) = \hat{c}_{\rm CC}^{\rm sr}(k) - \frac{\kappa_{\rm D}^2}{\rho}\, k^{-2} + \alpha_{\rm CC}\, k^3 \tag{23}$$

$$\hat{c}_{\rm NC}(k) = \hat{c}_{\rm NC}^{\rm sr}(k) + \alpha_{\rm NC}\, k^3 \tag{24}$$

where the inverse Debye screening length, $\kappa_{\rm D}$, is given by

$$\kappa_{\rm D}^2 = \frac{4\pi\beta e^2}{\epsilon}(\rho_a Z_a^2 + \rho_b Z_b^2), \tag{25}$$

the short-ranged parts of the direct correlation functions are given by

$$\hat{c}_{\rm NN}^{\rm sr}(k) = x_a^2\hat{c}_{aa}^{\rm sr}(k) + x_b^2\hat{c}_{bb}^{\rm sr}(k) + 2x_a x_b\hat{c}_{ab}^{\rm sr}(k) \tag{26}$$

$$\hat{c}_{\rm CC}^{\rm sr}(k) = x_a x_b[\hat{c}_{aa}^{\rm sr}(k) + \hat{c}_{bb}^{\rm sr}(k) - 2\hat{c}_{ab}^{\rm sr}(k)] \tag{27}$$

$$\hat{c}_{\rm NC}^{\rm sr}(k) = x_a[\hat{c}_{aa}^{\rm sr}(k) - \hat{c}_{ab}^{\rm sr}(k)] - x_b[\hat{c}_{bb}^{\rm sr}(k) - \hat{c}_{ab}^{\rm sr}(k)], \tag{28}$$

and equivalent expressions define $\alpha_{\rm NN}$, $\alpha_{\rm CC}$ and $\alpha_{\rm NC}$ in terms of the α_{ij}. Hence

$$\begin{aligned} S_{\rm NN}(k) &= \frac{\kappa_{\rm D}^2 + [1 - \rho\hat{c}_{\rm CC}^{\rm sr}(k)]k^2 - \rho\alpha_{\rm CC}\, k^5}{k^2 D(k)}, \\ \frac{S_{\rm CC}(k)}{x_a x_b} &= \frac{[1 - \rho\hat{c}_{\rm NN}^{\rm sr}(k)]k^2 - \rho\alpha_{\rm NN}\, k^5}{k^2 D(k)}, \\ \frac{S_{\rm NC}(k)}{x_a x_b} &= \frac{\rho\hat{c}_{\rm NC}^{\rm sr}(k)\, k^2 + \rho\alpha_{\rm NC}\, k^5}{k^2 D(k)} \end{aligned} \tag{29}$$

where

$$\begin{aligned} k^2 D(k) = {} & \kappa_{\rm D}^2[1 - \rho\hat{c}_{\rm NN}^{\rm sr}(k)] \\ & + [(1 - \rho\hat{c}_{\rm NN}^{\rm sr}(k))(1 - \rho\hat{c}_{\rm CC}^{\rm sr}(k)) - \rho_a\rho_b\,\hat{c}_{\rm NC}^{\rm sr}(k)^2]k^2 - \rho\,\alpha_{\rm NN}\,\kappa_{\rm D}^2\, k^3 \\ & - [\rho\alpha_{\rm NN}(1 - \rho\hat{c}_{\rm CC}^{\rm sr}(k)) + \rho\alpha_{\rm CC}(1 - \rho\hat{c}_{\rm NN}^{\rm sr}(k)) + 2\rho_a\rho_b\,\alpha_{\rm NC}\hat{c}_{\rm NC}^{\rm sr}(k)]k^5 \\ & + [\rho^2\alpha_{\rm NN}\alpha_{\rm CC} - \rho_a\rho_b\,\alpha_{\rm NC}^2]k^8. \end{aligned} \tag{30}$$

These formulae for the Bhatia–Thornton partial structure factors reduce to those previously obtained by Leote de Carvalho and Evans [22] for the case of a 1:1 binary ionic fluid where the ions have equal but opposite charges and there are no dispersion forces.

Note that if a liquid or glass can be fully described as a binary ionic system, i.e. as a two-component system comprising cations and anions, then it is usual to describe the fluctuations in number and charge density rather than the fluctuations in number density and concentration [30, 46]. With the imposition of overall charge neutrality $x_a Z_a + x_b Z_b = 0$ it

can be shown that charge–charge, $S_{ZZ}(k)$, and number–charge, $S_{NZ}(k)$, partial structure factors can be defined, where

$$S_{CC}(k) = x_a x_b S_{ZZ}(k), \tag{31}$$

$$S_{NC}(k) = (x_b/Z_a) S_{NZ}(k) \tag{32}$$

i.e. for purely ionic systems the two different descriptions are equivalent. The use of number density and concentration as the choice of variables is, however, more general, as it applies to non-ionic systems, and is therefore used throughout this manuscript.

2.3. Small-k behaviour of the partial structure factors

To deduce the small-k limits of the partial structure factors it is important to note that, following equation (20), $\hat{c}^{sr}_{NN}(k)$, $\hat{c}^{sr}_{CC}(k)$ and $\hat{c}^{sr}_{NC}(k)$ can each be expanded as a series containing even powers of k. Equation (30) can therefore be re-written as

$$k^2 D(k) = \kappa_D^2 (1 - \rho \hat{c}^{sr(0)}_{NN})[1 + \xi^{(2)} k^2 + \xi^{(3)} k^3 + \xi^{(4)} k^4 + \xi^{(5)} k^5 + O(k^6)] \tag{33}$$

where

$$\xi^{(2)} = \left[(1 - \rho \hat{c}^{sr(0)}_{NN})(1 - \rho \hat{c}^{sr(0)}_{CC}) - \rho \kappa_D^2 \hat{c}^{sr(2)}_{NN} - \rho_a \rho_b (\hat{c}^{sr(0)}_{NC})^2\right] \left[\kappa_D^2 (1 - \rho \hat{c}^{sr(0)}_{NN})\right]^{-1} \tag{34}$$

$$\xi^{(3)} = -\rho \alpha_{NN} / (1 - \rho \hat{c}^{sr(0)}_{NN}) \tag{35}$$

$$\xi^{(4)} = \Big[-\rho \kappa_D^2 \hat{c}^{sr(4)}_{NN} - \rho \hat{c}^{sr(2)}_{NN} (1 - \rho \hat{c}^{sr(0)}_{CC}) - \rho \hat{c}^{sr(2)}_{CC} (1 - \rho \hat{c}^{sr(0)}_{NN}) - 2\rho_a \rho_b \hat{c}^{sr(0)}_{NC} \hat{c}^{sr(2)}_{NC}\Big] \left[\kappa_D^2 (1 - \rho \hat{c}^{sr(0)}_{NN})\right]^{-1} \tag{36}$$

$$\xi^{(5)} = \Big[- \rho \alpha_{NN} (1 - \rho \hat{c}^{sr(0)}_{CC}) - \rho \alpha_{CC} (1 - \rho \hat{c}^{sr(0)}_{NN}) - 2\rho_a \rho_b \alpha_{NC} \hat{c}^{sr(0)}_{NC}\Big] \left[\kappa_D^2 (1 - \rho \hat{c}^{sr(0)}_{NN})\right]^{-1}. \tag{37}$$

At small k-values, it follows from a Taylor expansion of the denominator in equations (29) that

$$S_{NN}(k) = \frac{1}{(1 - \rho \hat{c}^{sr(0)}_{NN})} + \frac{\rho \kappa_D^2 \hat{c}^{sr(2)}_{NN} + \rho_a \rho_b (\hat{c}^{sr(0)}_{NC})^2}{\kappa_D^2 (1 - \rho \hat{c}^{sr(0)}_{NN})^2} k^2 + \frac{\rho \alpha_{NN}}{(1 - \rho \hat{c}^{sr(0)}_{NN})^2} k^3 + O(k^4), \tag{38}$$

$$\begin{aligned} \frac{S_{CC}(k)}{x_a x_b} = {} & \frac{k^2}{\kappa_D^2} - \frac{(1 - \rho \hat{c}^{sr(0)}_{NN})(1 - \rho \hat{c}^{sr(0)}_{CC}) - \rho_a \rho_b (\hat{c}^{sr(0)}_{NC})^2}{\kappa_D^4 (1 - \rho \hat{c}^{sr(0)}_{NN})} k^4 \\ & - \frac{\rho \hat{c}^{sr(4)}_{NN} + (1 - \rho \hat{c}^{sr(0)}_{NN}) \xi^{(4)} - \rho \hat{c}^{sr(2)}_{NN} \xi^{(2)} - (1 - \rho \hat{c}^{sr(0)}_{NN})(\xi^{(2)})^2}{\kappa_D^2 (1 - \rho \hat{c}^{sr(0)}_{NN})} k^6 \\ & + \frac{\rho \alpha_{CC} (1 - \rho \hat{c}^{sr(0)}_{NN})^2 + 2\rho_a \rho_b \alpha_{NC} \hat{c}^{sr(0)}_{NC} (1 - \rho \hat{c}^{sr(0)}_{NN}) + \rho \rho_a \rho_b \alpha_{NN} (\hat{c}^{sr(0)}_{NC})^2}{\kappa_D^4 (1 - \rho \hat{c}^{sr(0)}_{NN})^2} k^7 \\ & + O(k^8), \end{aligned} \tag{39}$$

$$\frac{S_{NC}(k)}{x_a x_b} = \frac{\rho \hat{c}^{sr(0)}_{NC}}{\kappa_D^2 (1 - \rho \hat{c}^{sr(0)}_{NN})} k^2 + \frac{\hat{c}^{sr(2)}_{NC} - \hat{c}^{sr(0)}_{NC} \xi^{(2)}}{\kappa_D^2 (1 - \rho \hat{c}^{sr(0)}_{NN})} \rho k^4 + \frac{\alpha_{NC} - \hat{c}^{sr(0)}_{NC} \xi^{(3)}}{\kappa_D^2 (1 - \rho \hat{c}^{sr(0)}_{NN})} \rho k^5 + O(k^6). \tag{40}$$

Note that equation (39) satisfies the Stillinger–Lovett conditions [47] in the limit as $k \to 0$, namely $S_{CC}(k)/x_a x_b \to (k/\kappa_D)^2$ and $S_{CC}(0) = 0$. It also follows from equations (8) and (38) that $S_{NN}(0) = \rho k_B T \chi_T = (1 - \rho \hat{c}_{NN}(0))^{-1}$, where $\hat{c}_{NN}(k = 0) = \hat{c}^{sr(0)}_{NN}$ (see equations (20) and (22)) and equation (40) gives $S_{NC}(0) = 0$ in agreement with equation (10).

Equations (38)–(40) show that the term with the lowest odd integer power of k for $S_{NN}(k)$, $S_{NC}(k)$ and $S_{CC}(k)$ is proportional to k^3, k^5 and k^7 respectively, in agreement with the results

of Kjellander and Forsberg [35]. If the dispersion forces are switched off in equation (17), $\alpha_{NN} = \alpha_{CC} = \alpha_{NC} = 0$ and the coefficients of these terms vanish. By comparison, if only the Coulomb interaction is switched off in equation (17), corresponding to a binary system with short-ranged repulsive forces and long-ranged dispersion forces, the term involving the inverse Debye screening length, κ_D, vanishes in equation (23) so that equations (29) and (30) remain valid provided κ_D is set equal to zero. The small-k behaviour of the Bhatia–Thornton partial structure factors can thus be deduced and the term proportional to k^3 is the lowest odd integer power of k for all three partial structure factors $S_{NN}(k)$, $S_{NC}(k)$ and $S_{CC}(k)$.

We note that the present theoretical scheme does not consider the effect of retardation, where the long range behaviour of the dispersion forces between polarizable ions, and hence the small-k properties of the partial structure factors, is affected by the finite velocity of propagation of the electromagnetic field [48]. The role of retardation in rare gas fluids, where the dispersion term in the pair potential eventually changes at large distances from having an r^{-6} to an r^{-7} dependence, is discussed by Reatto and Tau [49].

2.4. Symmetrical binary mixtures

For a symmetrical binary mixture, such as a molten alkali halide, $Z_a = -Z_b \equiv Z$ and $\rho_a = \rho_b = \rho/2$. The expressions previously found by Rovere *et al* [34] are then recovered from the first three terms in equation (38), the first two terms in equation (39) and the first term in equation (40). As noted by these authors, $S_{NN}(k)$ is the only Bhatia–Thornton partial structure factor which contains a term in k^3 and the only information on the ion polarizability that can be extracted by measuring the coefficient of this term is contained in α_{NN}. If, in addition, the short-ranged parts of the potentials are described by $\hat{c}^{sr}_{aa}(k) = \hat{c}^{sr}_{bb}(k) \neq \hat{c}^{sr}_{ab}(k)$ and the dispersion terms are described by $\alpha_{aa} = \alpha_{bb} \neq \alpha_{ab}$ it follows that $\hat{c}_{NC}(k) = 0$ since $\hat{c}^{sr}_{NC}(k) = 0$ and $\alpha_{NC} = 0$. Then equations (13), (14) and (15) simplify to

$$S_{NN}(k) = (1 - \rho\hat{c}_{NN}(k))^{-1} \tag{41}$$

$$S_{CC}(k)/x_a x_b = (1 - \rho\hat{c}_{CC}(k))^{-1} \tag{42}$$

$$S_{NC}(k)/x_a x_b = 0 \tag{43}$$

i.e. there is no correlation between the number density and concentration fluctuations. In the small-k regime the solution to these expressions is given by equations (38), (39) and (40), which become

$$S_{NN}(k) = \frac{1}{(1 - \rho\hat{c}^{sr(0)}_{NN})}\left[1 + \frac{\rho\hat{c}^{sr(2)}_{NN}}{(1 - \rho\hat{c}^{sr(0)}_{NN})}k^2 + \frac{\rho\alpha_{NN}}{(1 - \rho\hat{c}^{sr(0)}_{NN})}k^3 + O(k^4)\right] \tag{44}$$

$$\frac{S_{CC}(k)}{x_a x_b} = \frac{k^2}{\kappa_D^2} - (1 - \rho\hat{c}^{sr(0)}_{CC})\frac{k^4}{\kappa_D^4} + \left[\rho\hat{c}^{sr(2)}_{CC} + \frac{(1 - \rho\hat{c}^{sr(0)}_{CC})^2}{\kappa_D^2}\right]\frac{k^6}{\kappa_D^4} + \rho\alpha_{CC}\frac{k^7}{\kappa_D^4} + O(k^8) \tag{45}$$

with $S_{NC}(k) = 0$ at all k-values. On imposing the further restriction that $\hat{c}^{sr}_{aa}(k) = \hat{c}^{sr(k)}_{bb} = \hat{c}^{sr}_{ab}(k)$ and $\alpha_{aa} = \alpha_{bb} = \alpha_{ab}$, it follows that $\hat{c}^{sr}_{CC}(k) = 0$ and $\alpha_{CC} = 0$, such that (see equation (23)) $(1 - \rho\hat{c}_{CC}(k)) = 1 + \kappa_D^2/k^2$. Hence equation (42) becomes

$$\frac{S_{CC}(k)}{x_a x_b} = \frac{k^2}{\kappa_D^2}\left[1 + \frac{k^2}{\kappa_D^2}\right]^{-1} = \frac{k^2}{\kappa_D^2}\left[1 - \frac{k^2}{\kappa_D^2} + \frac{k^4}{\kappa_D^4} - \cdots\right] \tag{46}$$

where there are no odd powers of k.

If the Coulomb interaction is switched off in equation (17), corresponding to a binary system with short-ranged repulsive forces and long-ranged dispersion forces, the term involving the inverse Debye screening length, κ_D, vanishes in equation (23) so that equations (29) and (30)

remain valid provided κ_D is set equal to zero. By investigating the corresponding small-k behaviour of the Bhatia–Thornton partial structure factors when $\hat{c}^{sr}_{aa}(k) = \hat{c}^{sr}_{bb}(k) \neq \hat{c}^{sr}_{ab}(k)$ and $\alpha_{aa} = \alpha_{bb} \neq \alpha_{ab}$, it can be readily shown that $S_{NN}(k)$ is again given by equation (44), $S_{NC}(k) = 0$ at all k-values, whereas

$$\frac{S_{CC}(k)}{x_a x_b} = \frac{1}{(1-\rho\hat{c}^{sr(0)}_{CC})}\left[1 + \frac{\rho\hat{c}^{sr(2)}_{CC}}{(1-\rho\hat{c}^{sr(0)}_{CC})}\,k^2 + \frac{\rho\alpha_{CC}}{(1-\rho\hat{c}^{sr(0)}_{CC})}\,k^3 + O(k^4)\right]. \tag{47}$$

A random substitutional alloy corresponds to the further impositions $\hat{c}^{sr}_{aa}(k) = \hat{c}^{sr}_{bb}(k) = \hat{c}^{sr}_{ab}(k)$ and $\alpha_{aa} = \alpha_{bb} = \alpha_{ab}$, whereupon $\hat{c}^{sr}_{CC}(k) = 0$, $\alpha_{CC} = 0$ and $S_{CC}(k) = x_a x_b$ at all k-values.

2.5. Asymptotic decay of the pair correlation functions: no dispersion forces

The total pair correlation functions $h_{ij}(r)$ for the atomic species are given by the Fourier transform relations

$$rh_{ij}(r) = \frac{1}{2\pi^2}\int_0^\infty \mathrm{d}k\, k\,\hat{h}_{ij}(k)\sin(kr). \tag{48}$$

If dispersion forces are absent in the pair potentials defined by equation (17), the large-r behaviour of $rh_{ij}(r)$ can be found by using equations (4) and searching for the poles k_n (assumed to be simple) which satisfy $D(k_n) = 0$ in equation (5) and the corresponding residues R^{ij}_n of $k\hat{h}_{ij}(k)$ at k_n [21, 22, 25]. Irrespective of whether the pair potentials contain just the short-ranged parts or both the short-ranged and Coulomb parts

$$rh_{ij}(r) = \frac{1}{2\pi}\sum_n \exp(\sqrt{-1}\,k_n r)R^{ij}_n \tag{49}$$

i.e. the $rh_{ij}(r)$ can be written as a sum of terms which decay either purely exponentially, if the poles $k_n = \sqrt{-1}\,a_0$ are purely imaginary, or as exponentially damped oscillatory functions, if the pairs of poles $k_n = \pm a_1 + \sqrt{-1}\,a_0$ are complex. The term in equation (49) that gives rise to the slowest exponential decay will define the asymptotic behaviour of $rh_{ij}(r)$ as $r \to \infty$ and this corresponds to the leading order pole k_p, which has the smallest imaginary part. Since the denominator in equations (4) is the same for all of the $k\hat{h}_{ij}(k)$, it follows that the $rh_{ij}(r)$-functions will eventually decay exponentially with a common decay length given by a_0^{-1}, and, if there is also an oscillatory component, a common wavelength of oscillation given by $2\pi/a_1$. The exact form of the eventual decay will depend on the thermodynamic state of the system. The denominator in equations (13), (14) and (15) is also common for all of the Bhatia–Thornton partial structure factors and the corresponding $rh_{IJ}(r)$ are therefore expected to eventually decay either with a common decay length or with a common decay length and a common wavelength of oscillation.

When the leading order pole is purely imaginary, $k_p = \sqrt{-1}\,a_0$, the asymptotic form for a total pair correlation function for the atomic species is given by

$$rh_{ij}(r) \to \mathcal{A}_{ij}\exp(-a_0 r) \tag{50}$$

where the amplitudes are related by $\mathcal{A}_{aa}\mathcal{A}_{bb} = \mathcal{A}^2_{ab}$ [21, 22]. It follows by substituting in equations (12) that the asymptotic forms of the corresponding Bhatia–Thornton pair correlation functions are given by

$$rh_{NN}(r) \to \mathcal{A}_{NN}\exp(-a_0 r) \tag{51}$$

$$rh_{CC}(r) \to x_a x_b \mathcal{A}_{CC}\exp(-a_0 r) \tag{52}$$

$$rh_{NC}(r) \to \mathcal{A}_{NC}\exp(-a_0 r) \tag{53}$$

where the common decay length is given by a_0^{-1} and

$$\mathcal{A}_{\rm NN} = (x_a\mathcal{A}_{aa}^{1/2} + x_b\mathcal{A}_{bb}^{1/2})^2 \tag{54}$$

$$\mathcal{A}_{\rm CC} = (\mathcal{A}_{aa}^{1/2} - \mathcal{A}_{bb}^{1/2})^2 \tag{55}$$

$$\mathcal{A}_{\rm NC} = x_a(\mathcal{A}_{aa} - \mathcal{A}_{ab}) - x_b(\mathcal{A}_{bb} - \mathcal{A}_{ab}) \tag{56}$$

such that $\mathcal{A}_{\rm NN}\mathcal{A}_{\rm CC} = \mathcal{A}_{\rm NC}^2$. Alternatively, a pair of complex leading poles, $k_{\rm p} = \pm a_1 + \sqrt{-1}\,a_0$, give the asymptotic form

$$rh_{ij}(r) \to 2|\mathcal{A}_{ij}|\exp(-a_0 r)\cos(a_1 r - \theta_{ij}) \tag{57}$$

where $\mathcal{A}_{ij} = |\mathcal{A}_{ij}|\exp(-\sqrt{-1}\,\theta_{ij})$, the amplitudes are related by $|\mathcal{A}_{aa}||\mathcal{A}_{bb}| = |\mathcal{A}_{ab}|^2$ and the phases are related by $\theta_{aa} + \theta_{bb} = 2\theta_{ab}$ [21, 22]. For the Bhatia–Thornton pair correlation functions, it then follows by substituting in equations (12) that

$$rh_{\rm NN}(r) \to 2|\mathcal{A}_{\rm NN}|\exp(-a_0 r)\cos(a_1 r - \theta_{\rm NN}) \tag{58}$$

$$rh_{\rm CC}(r) \to 2x_a x_b|\mathcal{A}_{\rm CC}|\exp(-a_0 r)\cos(a_1 r - \theta_{\rm CC}) \tag{59}$$

$$rh_{\rm NC}(r) \to 2|\mathcal{A}_{\rm NC}|\exp(-a_0 r)\cos(a_1 r - \theta_{\rm NC}) \tag{60}$$

where the $\mathcal{A}_{IJ}$ given by equations (54)–(56) are now complex numbers with amplitudes related by $|\mathcal{A}_{\rm NN}||\mathcal{A}_{\rm CC}| = |\mathcal{A}_{\rm NC}|^2$ and phases related by $\theta_{\rm NN} + \theta_{\rm CC} = 2\theta_{\rm NC}$. The common decay length is given by a_0^{-1} and the common wavelength of the oscillations is given by $2\pi/a_1$. The crossover from pure exponential decay of the $rh_{IJ}(r)$ as described by equations (51)–(53) to exponentially damped oscillatory decay described by equations (58)–(60) defines a line in the $(\rho,\ T)$ plane known either as the Fisher–Widom line [21, 22, 24, 50] or as the Kirkwood line [22, 51, 52], depending on the mechanism by which crossover occurs. For a given temperature T, crossover to exponentially damped oscillatory decay often occurs for increasing number density ρ.

Note that in the special case when $\hat{c}_{\rm NC}(k) = 0$ (see section 2.4) the Bhatia–Thornton partial structure factors of equations (13), (14) and (15) reduce to equations (41), (42) and (43), i.e. the number density and concentration fluctuations become independent and the previous analysis, showing the communality between the asymptotic behaviour of the total pair correlation functions, no longer applies. In this case $rh_{\rm NN}(r)$ will, for example, decay more rapidly than $rh_{\rm CC}(r)$ if the imaginary part of the leading order pole $k_{\rm p}^{\rm NN}$ satisfying $(1 - \rho\hat{c}_{\rm NN}(k_{\rm p}^{\rm NN})) = 0$ is larger than the imaginary part of the leading order pole $k_{\rm p}^{\rm CC}$ satisfying $(1-\rho\hat{c}_{\rm CC}(k_{\rm p}^{\rm CC})) = 0$ [22]. For the restricted primitive model of a binary symmetrical electrolyte comprising charged hard spheres of equal diameter with $S_{\rm NC}(k) = 0$, the Fisher–Widom line is associated with the crossover in the asymptotic decay of the number density fluctuations whereas the Kirkwood line is associated with the crossover in the asymptotic decay of the concentration fluctuations, i.e. both crossover mechanisms occur in the same fluid [22].

2.6. Moments of the Bhatia–Thornton pair distribution functions

At small k-values, a series expansion of $\sin(kr)$ in equation (11) leads to the expression

$$S_{\rm NN}(k) - 1 = M_{\rm NN}^{(0)} + M_{\rm NN}^{(2)}k^2 + M_{\rm NN}^{(4)}k^4 + \cdots \tag{61}$$

where the running moments of $[g_{\rm NN}(r) - 1]$ are defined by [11]

$${}^{\rm run}M_{\rm NN}^{(2m)}(r_{\rm max}) = \int_0^{r_{\rm max}} {\rm d}r\rho_{\rm NN}^{(2m)}(r) \tag{62}$$

and the weighted pair distribution functions are given by

$$\rho_{\rm NN}^{(2m)}(r) = \frac{4\pi\rho(-1)^m}{(2m+1)!}\left[g_{\rm NN}(r) - 1\right]r^{2m+2} \tag{63}$$

with $m = 0, 1, 2, \ldots$. Hence the moments $M_{IJ}^{(2m)}$ of equation (61) are obtained by extending $r_{\max}$ to infinity in equation (62) and the coefficient of k^{2m} denotes the $(2m+2)$th moment of $[g_{\mathrm{NN}}(r) - 1]$. Equivalent expressions define the running moments ${}^{\mathrm{run}}M_{\mathrm{CC}}^{(2m)}(r_{\max})$ and ${}^{\mathrm{run}}M_{\mathrm{NC}}^{(2m)}(r_{\max})$ that correspond to $[S_{\mathrm{CC}}(k)/x_a x_b - 1]$ and $S_{\mathrm{NC}}(k)/x_a x_b$ together with the weighted pair distribution functions $\rho_{\mathrm{CC}}^{(2m)}(r)$ and $\rho_{\mathrm{NC}}^{(2m)}(r)$ that correspond to $g_{\mathrm{CC}}(r)$ and $g_{\mathrm{NC}}(r)$ respectively. Relevant expressions for some of the moments can be obtained by inspecting the coefficients of the even powers of k in equations (38)–(40) and in equations (44)–(47) (see also [11]), but care must be exercised since the moment expansion of equation (61) does not lead to odd powers of k. For instance, when dispersion forces are present the coefficients of even powers of k greater than the first odd power can differ substantially from the corresponding coefficients when dispersion forces are absent [53] (also see appendix A).

The contribution to a running second moment from the asymptotic form of the Bhatia–Thornton pair correlation functions given by equations (58)–(60) can be readily deduced by integration by parts. For example, when $[g_{\mathrm{NN}}(r) - 1]$ is given by equation (58) for $r \geqslant r_{\min}$, the large-r dependence of the running second moment is given by

$$4\pi\rho \int_{r_{\min}}^{r_{\max}} \mathrm{d}r\, [g_{\mathrm{NN}}(r) - 1] r^2 = 8\pi\rho \frac{|\mathcal{A}_{\mathrm{NN}}| \exp(-a_0 r_{\max})}{(a_0^2 + a_1^2)} \times \left[r_{\max}(a_1 \sin y - a_0 \cos y) + \frac{2a_0 a_1 \sin y + (a_1^2 - a_0^2)\cos y}{a_0^2 + a_1^2} \right] + \text{constant} \quad (64)$$

where $y \equiv a_1 r_{\max} - \theta_{\mathrm{NN}}$. Similar expressions hold for the running second moments of $g_{\mathrm{CC}}(r)$ and $g_{\mathrm{NC}}(r)$ i.e. when dispersion forces are absent the running second moments of the Bhatia–Thornton pair correlation functions should all decay exponentially at large r with a common decay length of a_0^{-1}.

The expression $1 + {}^{\mathrm{run}}M_{\mathrm{NN}}^{(0)}(r_{\max})$ is sometimes called the excess coordination [28]. This follows since the mean number of atoms in a sphere or radius $r_{\max}$ is given by $1 + 4\pi\rho \int_0^{r_{\max}} \mathrm{d}r\, r^2 g_{\mathrm{NN}}(r) = 1 + \bar{n}$, where $\bar{n} \equiv x_a \left(\bar{n}_a^a + \bar{n}_a^b\right) + x_b \left(\bar{n}_b^b + \bar{n}_b^a\right)$ is the mean coordination number irrespective of species type of an arbitrary atom chosen to be at the origin of coordinates and

$$\bar{n}_i^j = 4\pi\rho\, x_j \int_0^{r_{\max}} \mathrm{d}r\, r^2 g_{ij}(r) \quad (65)$$

is the mean coordination number of particles of type j contained within a spherical volume of radius $r_{\max}$ centred on a particle of type i [54]. For an ideal gas of the same number density ρ the mean number of particles contained in a sphere of the same radius is equal to $4\pi\rho \int_0^{r_{\max}} \mathrm{d}r\, r^2$. Hence $1 + 4\pi\rho \int_0^{r_{\max}} \mathrm{d}r\, r^2 [g_{\mathrm{NN}}(r) - 1]$ is a measure of the deviation from ideal gas behaviour in the mean number of particles contained within a sphere of radius $r_{\max}$. Often, a local positive deviation from ideal gas behaviour owing to a peak in $g_{\mathrm{NN}}(r)$ is followed by a negative deviation and the measured excess coordination can be a strongly oscillatory function [11, 28]. Note that as $r_{\max} \to \infty$, equations (8) and (61) show that the limiting value of the excess coordination is given by $1 + M_{\mathrm{NN}}^{(0)} = S_{\mathrm{NN}}(0) = \rho k_{\mathrm{B}} T \chi_T + \delta^2 S_{\mathrm{CC}}(0)$, i.e. diffraction experiments are generally sensitive to fluctuations in the number density of particles, which depend *inter alia* on the compressibility of the system.

The measured function ${}^{\mathrm{run}}M_{\mathrm{CC}}^{(0)}(r_{\max})$ can also be strongly oscillatory [11]. Consider, for example, the case of a binary ionic system. If chemical species a with charge Z_a is chosen to be at the origin of coordinates, the mean charge in a surrounding sphere of radius r_a is given by $Z_a + \bar{n}_a^a Z_a + \bar{n}_a^b Z_b$ and will cancel if

$$Z_a + 4\pi\rho \int_0^{r_a} \mathrm{d}r\, r^2 \left[x_a Z_a g_{aa}(r) + x_b Z_b g_{ab}(r) \right] = 0. \quad (66)$$

Alternatively, if chemical species b with charge Z_b is at the origin, the mean charge in a surrounding sphere of radius r_b is given by $Z_b + \bar{n}_b^b Z_b + \bar{n}_b^a Z_a$ and will cancel if

$$Z_b + 4\pi\rho \int_0^{r_b} \mathrm{d}r\, r^2 \left[x_b Z_b g_{bb}(r) + x_a Z_a g_{ba}(r)\right] = 0 \tag{67}$$

where $g_{ab}(r) = g_{ba}(r)$. For a symmetrical molten salt with $x_a = x_b = 1/2$, $Z_a = -Z_b$ and $g_{aa}(r) = g_{bb}(r)$ [30] it follows that equations (66) and (67) will hold when $r_a = r_b \equiv r'$. Hence by subtracting these equations and by using the definition of $g_{\mathrm{CC}}(r)$ given by equations (12) it follows that

$${}^{\mathrm{run}}M_{\mathrm{CC}}^{(0)}(r') = 4\pi\rho \int_0^{r'} \mathrm{d}r\, r^2 g_{\mathrm{CC}}(r) = -1 \tag{68}$$

which becomes the first Stillinger–Lovett [47] condition when $r' \to \infty$, i.e. for an ionic system $M_{\mathrm{CC}}^{(0)} = S_{\mathrm{CC}}(0)/x_a x_b - 1 = -1$. As layers of alternate charge are built around a charged species at the origin, it is feasible that equation (68) will hold for a set of increasingly large values of r', corresponding to a tendency for local charge neutrality, such that $1 + {}^{\mathrm{run}}M_{\mathrm{CC}}^{(0)}(r_{\max})$ oscillates about zero as $r_{\max}$ is made increasingly large. For the restricted primitive model of a symmetrical electrolyte in which the ions are equi-sized hard spheres of diameter d with $\phi_{ij}(r) = +\infty$ for $r \leqslant d$ and $\phi_{ij}(r) = Z_i Z_j e^2/\epsilon r$ for $r > d$, oscillations in the charge density will occur if $\kappa_{\mathrm{D}} d \geqslant \sqrt{6}$ [30, 55]. Estimates of the so-called Kirkwood line in the phase diagram for the restricted primitive model of a symmetrical electrolyte, marking a change from pure exponential decay to exponentially damped oscillatory decay of the charge-density fluctuations, are given in [22].

2.7. *Asymptotic decay of the pair correlation functions: dispersion forces*

If dispersion forces are present in the pair potentials defined by equation (17), the analysis given in section 2.5 is no longer valid [23] and it is the term with the lowest odd integer power of k in equation (38), (39) or (40) that is expected to give rise to the longest-ranged behaviour in r-space [23, 35, 36]. Provided $\hat{f}_{IJ}(k) \equiv k\hat{h}_{IJ}(k)$ and its derivatives exist as ordinary functions for $k \geqslant 0$ and are well behaved at infinity it can be shown that at large r [56]

$$\begin{aligned} 2\pi^2 r h_{IJ}(r) &= \int_0^\infty \mathrm{d}k\, k\, \hat{h}_{IJ}(k) \sin(kr) \\ &\sim \frac{\hat{f}_{IJ}(0)}{r} - \frac{\hat{f}_{IJ}^{\mathrm{ii}}(0)}{r^3} + \frac{\hat{f}_{IJ}^{\mathrm{iv}}(0)}{r^5} - \frac{\hat{f}_{IJ}^{\mathrm{vi}}(0)}{r^7} + \frac{\hat{f}_{IJ}^{\mathrm{viii}}(0)}{r^9} - \cdots \end{aligned} \tag{69}$$

where the superscripts refer to successive derivatives of $\hat{f}_{IJ}(k)$ with respect to k as evaluated at $k = 0$. By considering only those terms in equations (38)–(40) that involve the lowest odd integer power of k it follows that

$$rh_{\mathrm{NN}}(r) \to \frac{12\,\mathcal{C}^{(3)}}{\pi^2}\frac{1}{r^5} \tag{70}$$

$$rh_{\mathrm{CC}}(r) \to \frac{20\,160\,\mathcal{C}^{(7)}}{\pi^2}\frac{1}{r^9} \tag{71}$$

$$rh_{\mathrm{NC}}(r) \to -\frac{360\,\mathcal{C}^{(5)}}{\pi^2}\frac{1}{r^7} \tag{72}$$

where $\mathcal{C}^{(3)}$, $\mathcal{C}^{(5)}$ and $\mathcal{C}^{(7)}$ give the coefficients of the k^3, k^5 and k^7 terms in equations (38), (40) and (39) respectively. These expressions, which were first obtained by Kjellander and Forsberg [35], show that the dispersion forces result in a power-law decay of the total pair

correlation functions, as opposed to the exponential decay given by equations (51)–(53) or equations (58)–(60). The power-law terms should, therefore, determine the ultimate large-r decay of the Bhatia–Thornton pair correlation functions. If only the Coulomb interaction is switched off in equation (17), corresponding to a binary system with short-ranged repulsive forces and long-ranged dispersion forces, the term proportional to k^3 is the lowest odd integer power of k for $S_{\mathrm{NN}}(k)$, $S_{\mathrm{NC}}(k)$ and $S_{\mathrm{CC}}(k)$ (see section 2.3) and all of the corresponding $rh_{IJ}(r)$ pair correlation functions should ultimately decay with an r^{-5} dependence. The effect of including ion-induced dipole interactions in the pair potential of equation (17) is briefly discussed in appendix A.

For some systems at high densities it is found that the total pair correlation functions can be accurately represented over a wide r-range by summing the results obtained from a complex leading order pole and a power-law term obtained from the dispersion forces [21, 23]. A convenient reference point for analysing the r-dependence of the Bhatia–Thornton pair correlation functions obtained from experiment might therefore be obtained by combining the results of equations (58)–(60) with the results of equations (70)–(72) to give

$$rh_{\mathrm{NN}}(r) \to 2|\mathcal{A}_{\mathrm{NN}}|\exp(-a_0 r)\cos(a_1 r - \theta_{\mathrm{NN}}) + \frac{12\,\mathcal{C}^{(3)}}{\pi^2}\frac{1}{r^5} \tag{73}$$

$$rh_{\mathrm{CC}}(r) \to 2x_a x_b|\mathcal{A}_{\mathrm{CC}}|\exp(-a_0 r)\cos(a_1 r - \theta_{\mathrm{CC}}) + \frac{20\,160\,\mathcal{C}^{(7)}}{\pi^2}\frac{1}{r^9} \tag{74}$$

$$rh_{\mathrm{NC}}(r) \to 2|\mathcal{A}_{\mathrm{NC}}|\exp(-a_0 r)\cos(a_1 r - \theta_{\mathrm{NC}}) - \frac{360\,\mathcal{C}^{(5)}}{\pi^2}\frac{1}{r^7} \tag{75}$$

although it is not clear that the relations $|\mathcal{A}_{\mathrm{NN}}||\mathcal{A}_{\mathrm{CC}}| = |\mathcal{A}_{\mathrm{NC}}|^2$ and $\theta_{\mathrm{NN}} + \theta_{\mathrm{CC}} = 2\theta_{\mathrm{NC}}$ will remain valid as they were derived for the case when dispersion forces are absent.

3. Experimental results

The Bhatia–Thornton partial structure factors, $S_{IJ}(k)$, can be measured by using the method of isotopic substitution in neutron diffraction [9], the method of isomorphic substitution in neutron diffraction [57], or the method of combining neutron and x-ray diffraction patterns [40]. For example, if neutron diffraction experiments are made on three samples of a binary liquid or glass, which are identical in every respect except for the isotopic composition of chemical species b, then the corresponding total structure factors of equation (7) can be represented in matrix notation by

$$\begin{bmatrix} F(k) \\ {}'F(k) \\ {}''F(k) \end{bmatrix} = \begin{bmatrix} \langle f\rangle^2 & x_a x_b(f_a - f_b)^2 & 2\langle f\rangle(f_a - f_b) \\ \langle {}'f\rangle^2 & x_a x_b(f_a - {}'f_b)^2 & 2\langle {}'f\rangle(f_a - {}'f_b) \\ \langle {}''f\rangle^2 & x_a x_b(f_a - {}''f_b)^2 & 2\langle {}''f\rangle(f_a - {}''f_b) \end{bmatrix} \begin{bmatrix} S_{\mathrm{NN}}(k) - 1 \\ S_{\mathrm{CC}}(k)/x_a x_b - 1 \\ S_{\mathrm{NC}}(k) \end{bmatrix}$$
$$\equiv \begin{bmatrix} a_{11} & a_{12} & a_{13} \\ a_{21} & a_{22} & a_{23} \\ a_{31} & a_{32} & a_{33} \end{bmatrix} \begin{bmatrix} S_{\mathrm{NN}}(k) - 1 \\ S_{\mathrm{CC}}(k)/x_a x_b - 1 \\ S_{\mathrm{NC}}(k) \end{bmatrix} \tag{76}$$

where f_b, ${}'f_b$ and ${}''f_b$ represent the different coherent scattering lengths of chemical species b and the average scattering lengths $\langle f\rangle$, $\langle {}'f\rangle$ and $\langle {}''f\rangle$ are evaluated accordingly. The $S_{IJ}(k)$ can be obtained by inverting this matrix to give

$$\begin{bmatrix} S_{\mathrm{NN}}(k) - 1 \\ S_{\mathrm{CC}}(k)/x_a x_b - 1 \\ S_{\mathrm{NC}}(k) \end{bmatrix} = [A]^{-1} \begin{bmatrix} F(k) \\ {}'F(k) \\ {}''F(k) \end{bmatrix} \tag{77}$$

where $[A]$ is the matrix represented by the coefficients a_{lm} $(l, m = 1, 2, 3)$ in equation (76). The determinant $|A|_{\mathrm{n}}$, normalized by dividing each row l of $[A]$ by $(\sum_m a_{lm}^2)^{1/2}$, is a measure

of the conditioning of the matrix [58], i.e. of the robustness in the determination of the $S_{IJ}(k)$ resulting from the scattering length 'contrast' between the measured total structure factors. In the present paper, attention is focused on the most recently measured data sets for which advances in neutron diffraction instrumentation have enabled the $S_{IJ}(k)$ to be obtained by direct inversion of the scattering matrix without the application of any additional constraints [40]. Unfortunately, this has precluded a detailed investigation of relatively simple molten salts such as NaCl [59], $CaCl_2$ [60] and $SrCl_2$ [61], although the Bhatia–Thornton partial structure factors for various molten 2:1 systems are described in [9]. The systems investigated include l-CuSe [62] and l-GeSe [63, 64], which are molten semiconductors, l-Ag_2Se [65], which melts from a super-ionic phase, and l-$GeSe_2$ [66, 67], which is a network glass forming semiconductor, where the prefix before the chemical formulae denotes the liquid phase. The network forming glasses g-$GeSe_2$ [68, 69], g-$ZnCl_2$ [10] and g-GeO_2 [12] were also investigated where the prefix denotes a glass. For these systems, the conditioning of the Bhatia–Thornton partial structure factors is better than for the corresponding Faber–Ziman partial structure factors.

The instrumentation used for the diffraction experiments did not access k-values of $\leqslant$0.2–0.3 Å^{-1} or $\leqslant$0.4–0.45 Å^{-1}, depending on whether the incident neutron wavelength was 0.7 or 0.5 Å respectively (see below). In consequence, the measured Bhatia–Thornton partial structure factors were extrapolated to $k = 0$ by plotting either $[S_{\rm NN}(k) - 1]$, $[S_{\rm CC}(k)/x_a x_b - 1]$ or $S_{\rm NC}(k)/x_a x_b$ versus k^2 and fitting a straight line at small k. The corresponding total pair correlation functions were then obtained by (i) spline-fitting or (ii) not spline fitting the partial structure factors and then Fourier transforming after the application of a Lorch [70] modification function $M(k) = \sin(\pi k/k_{\rm max})/(\pi k/k_{\rm max})$, where $k_{\rm max}$ is the maximum measured k-value (see appendix B). Application of this modification function gives smoother pair correlation functions at all r-values by comparison with the use of a step modification function, $M(k) = 1$ for $k \leqslant k_{\rm max}$ and $M(k) = 0$ for $k > k_{\rm max}$, but leads to a loss in resolution of the first peaks in r-space. Procedure (i) also leads to smoother pair correlation functions than procedure (ii) but can lead to spurious features at the largest r-values. To avoid the latter and to identify a suitable range for fitting, a comparison was made between the plots of $\ln|rh_{IJ}(r)|$ versus r obtained from both procedures. The $rh_{IJ}(r)$-functions obtained from procedure (i) were then fitted at the largest r-values by using equations (58)–(60). Finally, the fitted parameters were used to calculate the corresponding $rh_{IJ}(r)$-functions at all r-values.

The extrapolation procedure adopted at small k, which assumes quadratic behaviour of the partial structure factors, is somewhat arbitrary, since coefficients with odd powers of k can also occur in the small-k region of a partial structure factor (section 2.3). In the case of ionic systems, some justification for assuming a quadratic dependence arises from the small magnitude of the dispersion terms relative to the Coulomb terms in equation (17). For instance, in molecular dynamics simulations of molten $ZnCl_2$ using a polarizable ion model [8], the parameters used for the pair potentials give a Coulomb energy that is $\approx$142 times greater than the dispersion energy for the Zn–Cl pair at a typical nearest-neighbour separation of 5 au (i.e. 2.65 Å). By comparison, the same model when applied to molten $GeSe_2$ corresponds to a Coulomb energy for the Ge–Se pair that is $\approx$16 times greater than the dispersion energy at the same separation [8]. The small-k extrapolation procedure will not, therefore, necessarily produce $rh_{IJ}(r)$-functions that have the correct asymptotic properties. However, several theoretical and Monte Carlo studies of systems described by simple model pair potentials show that the asymptotic behaviour described by equations (50) and (57) can also provide an accurate description of the total pair correlation functions at distances much shorter than the longest range [21–23, 25, 26]. Since the features observed at shorter distances are less sensitive to the details of any small-k fitting procedure, the parameters extracted from the fits to

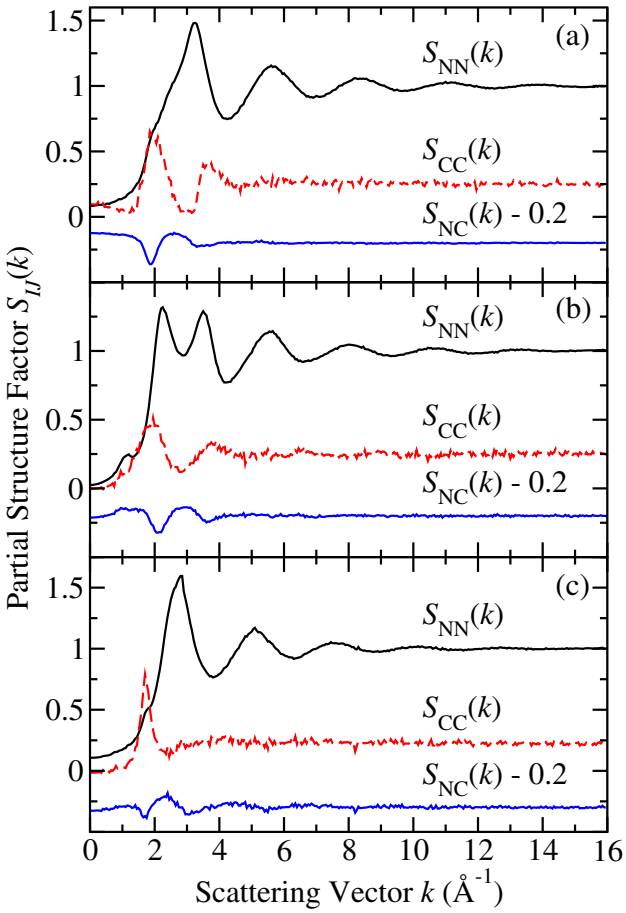

Figure 1. The measured Bhatia–Thornton partial structure factors $S_{IJ}(k)$ for (a) l-CuSe [62], (b) l-GeSe [63, 64] and (c) l-Ag_2Se [65]. The statistical uncertainties are represented by the scatter in the data points.

the $rh_{IJ}(r)$-functions will be most robust when the asymptotic behaviour extends to relatively small r-values for the systems studied experimentally.

The measured $S_{IJ}(k)$-functions are shown in figures 1–3 and the corresponding $rh_{IJ}(r)$-functions are shown in figures 4–6 together with the functions obtained by fitting the $rh_{IJ}(r)$ at large r and extrapolating to all r-values. For each $rh_{IJ}(r)$-function, the fitted parameters, the range used for the fits and the R^2 goodness-of-fit parameter are summarized in table 1. The decay length a_0^{-1} was also obtained from the same data sets in the same r-space range by plotting $\ln|rh_{IJ}(r)|$ versus r and fitting the repeated maxima to the straight line $\ln|rh_{IJ}(r)| = -a_0 r$ +constant (see [12]). The corresponding a_0-values are also given in table 1.

The values of the measured decay lengths a_0^{-1} will represent lower limits owing to the k-space resolution function of the diffractometer. For example, a simple Gaussian resolution function leads to an exponential damping of the measured $rh_{IJ}(r)$-functions (see appendix C). In practice, the resolution function of a diffractometer has a more complicated k-dependence and a suitable correction could be made if sufficient information is known about the experimental set-up (see e.g. [71]). This is not, however, the case for most of the measured diffraction patterns, so a resolution function correction was not attempted. Nevertheless, with the exception of glassy $ZnCl_2$ and GeO_2, all of the data sets were measured using the same diffractometer (D4B at the Institut Laue–Langevin [72]) with an incident neutron wavelength of

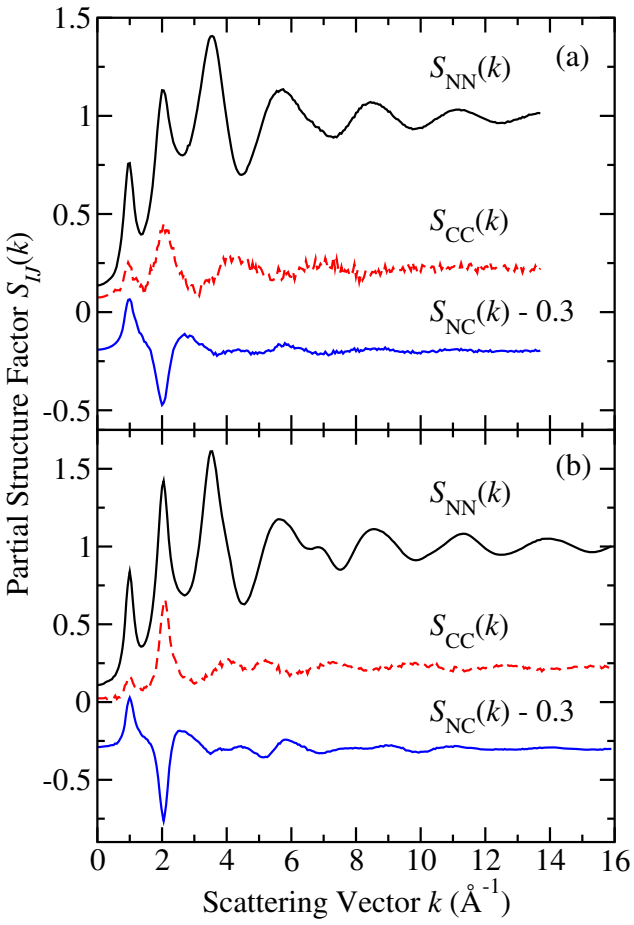

Figure 2. The measured Bhatia–Thornton partial structure factors $S_{IJ}(k)$ for (a) l-$GeSe_2$ [66, 67] and (b) g-$GeSe_2$ [68, 69]. The statistical uncertainties are represented by the scatter in the data points.

≈ 0.7 Å and comparable resolution functions are to be expected. The data sets for glassy $ZnCl_2$ and GeO_2 were measured using the new D4C diffractometer at the Institut Laue–Langevin [73] with an incident neutron wavelength of $\approx$0.5 Å under very similar experimental conditions, i.e. the resolution function is the same for both of these glasses.

4. Discussion

4.1. Description of the measured data sets using simple theory

The results for glassy $GeSe_2$, $ZnCl_2$ and GeO_2 show that an exponentially damped oscillatory function can be used to account for the large-r behaviour of all the measured $rh_{IJ}(r)$-functions. For $rh_{CC}(r)$ and $rh_{NC}(r)$ this damped oscillatory function also provides a good representation of the measured data at intermediate values, as small as $\approx$3 Å in the case of $rh_{CC}(r)$ for g-GeO_2 (figures 5(b) and 6). It is consequently easier to fit these data sets than those for $rh_{NN}(r)$. In reciprocal space (figures 2(b) and 3), $S_{CC}(k)$ and $S_{NC}(k)$ have sharp principal peaks and are otherwise relatively featureless compared to $S_{NN}(k)$, which has the 'three-peak' character of the diffraction pattern measured for many network forming glasses [74]. Hence, although $S_{NN}(k)$ also has a sharp principal peak, the corresponding r-space function shows more complexity and in the case of g-GeO_2, where the intensity of the principal peak is relatively small, it is

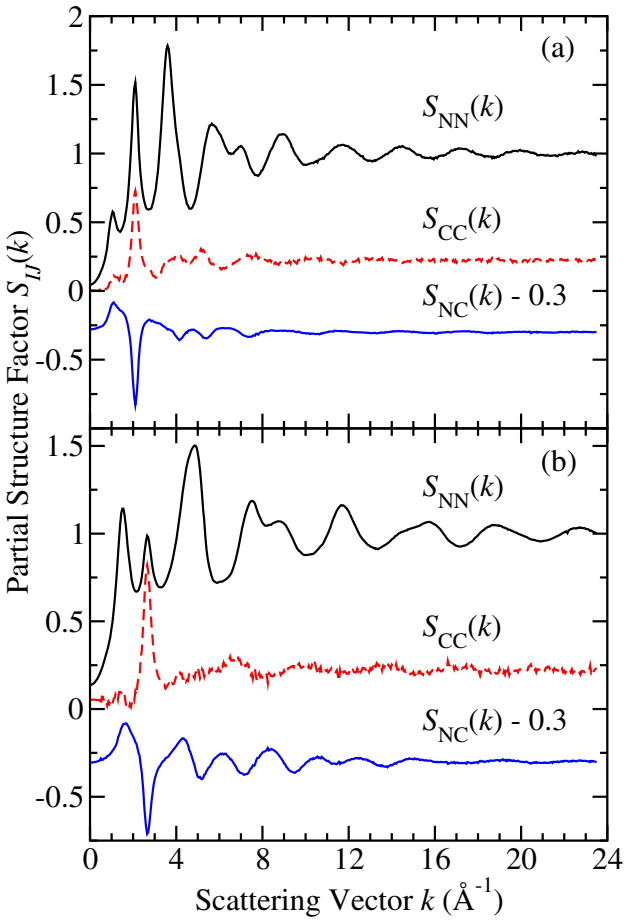

Figure 3. The measured Bhatia–Thornton partial structure factors $S_{IJ}(k)$ for (a) g-$ZnCl_2$ [10] and (b) g-GeO_2 [12]. The statistical uncertainties are represented by the scatter in the data points.

particularly difficult to fit $rh_{NN}(r)$ at large r by using equation (58). A partial structure factor $S_{IJ}(k)$ that is dominated by a single sharp peak is expected to give rise to damped oscillatory behaviour in real space; e.g., a Lorentzian peak centred at k_{PP} with a full width at half maximum of $2a_0$ will give rise to an exponentially damped oscillatory function with a wavelength given by $2\pi/k_{PP}$ and a decay length given by a_0^{-1} [3].

As shown in table 1, the large-r behaviour of the $rh_{IJ}(r)$-functions for each glass, which is sometimes called the extended-range ordering, is described by a common wavelength of oscillation $2\pi/a_1 \approx 2\pi/k_{PP}$ and a roughly common decay length a_0^{-1} that takes approximate values of 4.8 Å for g-$GeSe_2$, 5.1 Å for g-$ZnCl_2$ and 3.8 Å for g-GeO_2. The relation $|\mathcal{A}_{NN}||\mathcal{A}_{CC}| = |\mathcal{A}_{NC}|^2$ of section 2.5 does not hold for any of the glasses although the relation $\theta_{NN} + \theta_{CC} = 2\theta_{NC}$ of section 2.5 does hold, within the experimental error, for glassy $ZnCl_2$ and $GeSe_2$. In the case of the most recently measured data sets, i.e. those for $ZnCl_2$ and GeO_2, the $rh_{IJ}(r)$ were also fitted by using equations (73)–(75). The fits were marginally improved but the same values for a_0 and a_1 were obtained within the experimental error. This result might be anticipated since the $rh_{IJ}(r)$-functions were obtained by inverting partial structure factors that were extrapolated to small k-values by assuming a quadratic dependence and it is precisely the behaviour of the $S_{IJ}(k)$ in this k-space region that dictates the ultimate decay of the pair correlation functions in real space. An accurate measurement of the $S_{IJ}(k)$ at small k-values

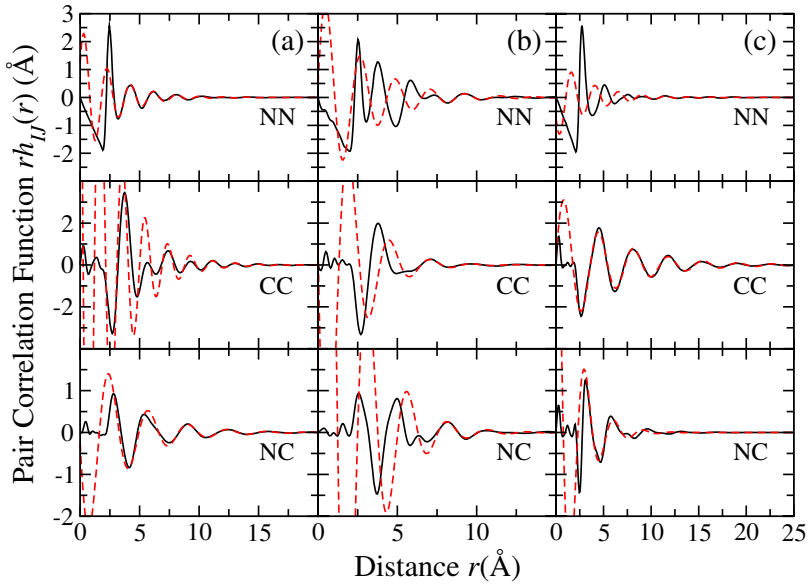

Figure 4. The solid curves show the measured Bhatia–Thornton pair correlation functions $rh_{IJ}(r)$ for l-CuSe (column (a)), l-GeSe (column (b)) and l-Ag_2Se (column (c)). The broken (red) curves show the fits to the $rh_{IJ}(r)$-functions at large r (see table 1) as extrapolated to all r-values.

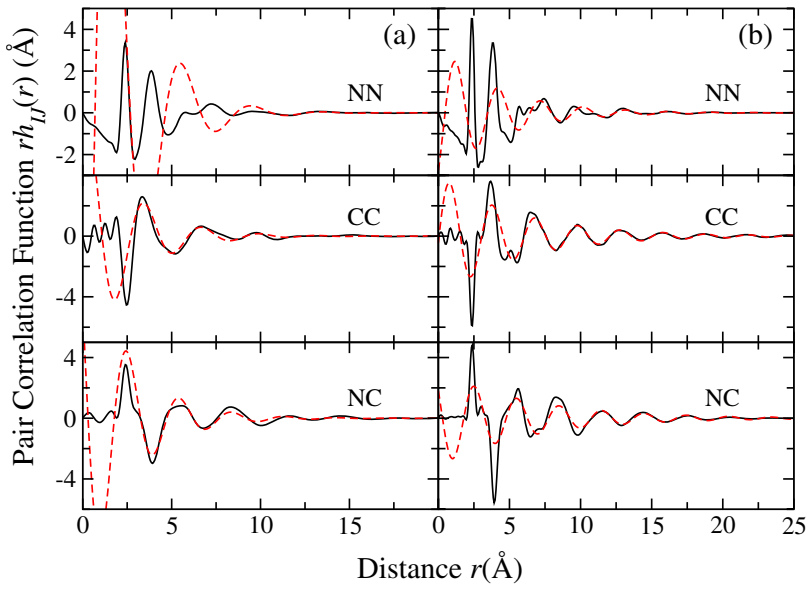

Figure 5. The solid curves show the measured Bhatia–Thornton pair correlation functions $rh_{IJ}(r)$ for liquid $GeSe_2$ (column (a)) and glassy $GeSe_2$ (column (b)). The broken (red) curves show the fits to the $rh_{IJ}(r)$-functions at large r (see table 1) as extrapolated to all r-values.

is therefore required in order to fully appreciate the effect of dispersion forces on the measured pair correlation functions at large r.

Nevertheless, although the fitted amplitudes and phases do not necessarily satisfy the relations $|\mathcal{A}_{NN}||\mathcal{A}_{CC}| = |\mathcal{A}_{NC}|^2$ and $\theta_{NN} + \theta_{CC} = 2\theta_{NC}$ given in section 2.5, it appears that

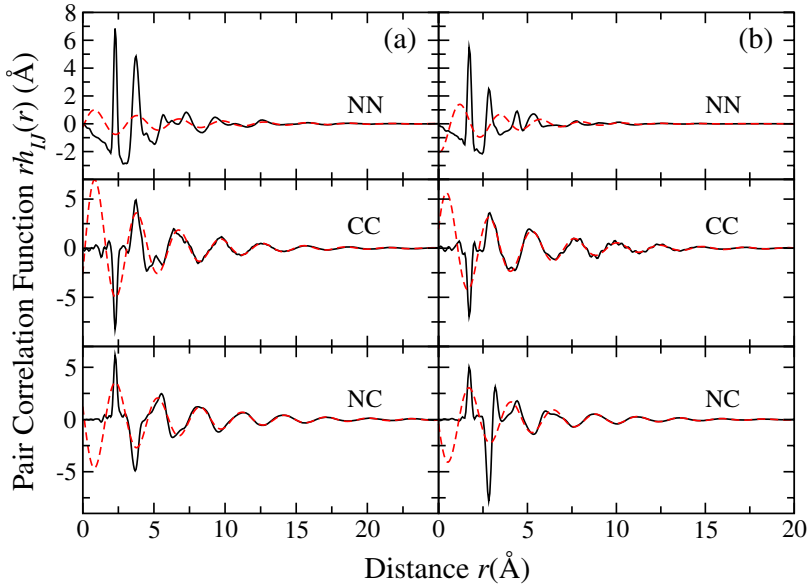

Figure 6. The solid curves show the measured Bhatia–Thornton pair correlation functions $rh_{IJ}(r)$ for glassy $ZnCl_2$ (column (a)) and glassy GeO_2 (column (b)). The broken (red) curves show the fits to the $rh_{IJ}(r)$-functions at large r (see table 1) as extrapolated to all r-values.

Table 1. Parameters obtained by fitting the Bhatia–Thornton pair correlation functions $rh_{IJ}(r)$ by using equations (58)–(60).

System	IJ	a_0 (Å^{-1})	a_0^{a} (Å^{-1})	a_1 (Å^{-1})	k_{PP} (Å^{-1})	A_{IJ}^{b} (Å)	θ_{IJ} (rad)	R^2	Range (Å)
l-CuSe	NN	0.40(1)	0.38(4)	3.22(1)	3.24(1)	2.6(2)	−1.07(6)	0.98	3.7–10.9
	CC	0.42(2)	0.41(7)	3.31(2)	1.86(3)	23(6)	0.7(2)	0.96	10.7–16.3
	NC	0.297(7)	0.32(2)	1.889(7)	1.87(1)	2.9(2)	1.66(7)	0.98	8.3–16.8
l-GeSe	NN	0.37(2)	0.39(3)	2.86(2)	2.24(2)	4.0(7)	−1.4(2)	0.98	7.7–11.2
	CC	0.58(2)	0.35(8)	2.42(2)	1.95(5)	17(3)	−4.8(1)	0.96	6.5–13.4
	NC	0.53(2)	0.7(2)	2.48(2)	2.09(3)	19(4)	4.8(2)	0.98	7.5–11.5
l-Ag_2Se	NN	0.30(2)	0.4(1)	2.54(2)	2.83(2)	1.5(3)	2.1(2)	0.97	9.7–14.4
	CC	0.187(6)	0.21(3)	1.718(5)	1.71(1)	3.6(2)	−1.49(5)	0.98	7.2–16.3
	NC	0.53(4)	0.43(2)	2.05(3)	1.75(5)	7(2)	0.0(1)	0.90	3.8–10.5
l-$GeSe_2$	NN	0.49(4)	—	1.58(3)	2.02(1)	37(18)	3.6(2)	0.85	10.5–18.8
	CC	0.41(2)	0.34(5)	1.94(2)	1.97(3)	8.9(8)	−0.5(1)	0.91	2.9–12.7
	NC	0.41(2)	0.27(3)	2.13(2)	2.01(2)	12(1)	0.93(7)	0.92	3.3–17.4
g-$GeSe_2$	NN	0.24(2)	0.29(5)	2.10(2)	2.04(1)	3(1)	−2.6(4)	0.95	15.6–21.0
	CC	0.180(4)	0.185(9)	2.093(4)	2.09(1)	4.0(2)	−1.68(4)	0.98	7.6–19.4
	NC	0.158(9)	0.21(3)	2.104(8)	2.05(1)	3.1(4)	−5.3(1)	0.96	10.8–19.8
g-$ZnCl_2$	NN	0.17(1)	0.20(2)	2.11(1)	2.09(1)	1.1(2)	−1.8(2)	0.91	15.2–25.6
	CC	0.225(5)	0.204(7)	2.133(5)	2.10(1)	8.5(4)	−1.89(5)	0.97	7.7–26.9
	NC	0.183(4)	0.184(7)	2.119(3)	2.10(1)	5.4(3)	1.34(5)	0.98	10.5–25.5
g-GeO_2	NN	0.33(3)	0.27(4)	2.78(3)	2.67(1)	2.1(8)	2.8(4)	0.86	12.3–19.9
	CC	0.24(1)	0.23(2)	2.62(1)	2.65(1)	6.3(5)	−1.26(7)	0.94	4.7–15.4
	NC	0.250(5)	0.26(1)	2.654(5)	2.66(1)	4.7(2)	1.66(5)	0.99	7.1–16.6

[a] From a straight-line fit to the maxima in $\ln|rh_{IJ}(r)|$ versus r.
[b] $A_{NN} \equiv 2|\mathcal{A}_{NN}|$, $A_{CC} \equiv 2x_a x_b|\mathcal{A}_{CC}|$ and $A_{NC} \equiv 2|\mathcal{A}_{NC}|$.

a simple ionic model might provide a suitable starting point for understanding the extended-range ordering in these network glasses. Indeed, a *rudimentary* representation of the structure of these materials can be provided within the framework of an ionic model. A complication is, however, provided by the appearance of an FSDP, since this feature is usually taken to be a signature that directional bonding is an important feature of the inter-atomic interactions [9]. In consequence, it is necessary to go beyond a rigid ion model by the inclusion of polarization effects such as induced dipoles for systems like $ZnCl_2$ [8, 75, 76], and first principles molecular dynamics simulations are required for systems like $GeSe_2$ to accurately reproduce important features such as homopolar bonds and the FSDP in $S_{CC}(k)$ [7, 69, 77–80]. It is notable that the principal peak gains in importance relative to the FSDP when e.g. the basic tetrahedral structural motifs are more densely packed, as for $ZnCl_2$ compared with GeO_2 or SiO_2 [12], or when systems such as glassy $GeSe_2$ [81] and GeO_2 [82] are compressed. Indeed, an interplay between the ordering on these length scales may help to account for the relative fragility of 2:1 network glass forming systems [12].

By comparison with the glass, it proved problematic to adequately fit the measured $rh_{IJ}(r)$ for the liquid phase of $GeSe_2$ by using equations (58)–(60), especially in the case of $rh_{NN}(r)$, and the fitted functions do not provide a good representation of the measured $rh_{IJ}(r)$ over a wide r-range (figure 5(a)). The oscillations in $rh_{IJ}(r)$ are less pronounced for the liquid compared to the glass and, with the exception of the FSDP, the features in the corresponding $S_{IJ}(k)$ for the liquid are broader (figure 2). For the liquid, the principal peak in all of the $S_{IJ}(k)$ occurs at the same position $k_{PP} \approx 2$ Å^{-1} and, at least for $rh_{CC}(r)$ and $rh_{NC}(r)$, the fitted wavelength of the oscillations is again given by $2\pi/a_1 \approx 2\pi/k_{PP}$ (table 1).

By contrast to the network glasses and liquid $GeSe_2$, the principal peaks in $S_{NN}(k)$ and $S_{CC}(k)$ for l-Ag_2Se occur at substantially different positions of 2.83(2) and 1.71(1) Å^{-1} respectively (figure 1(c)). For this liquid, an exponentially damped oscillatory function accounts for the large-r behaviour of $rh_{NN}(r)$ and $rh_{CC}(r)$ and, in the case of $rh_{CC}(r)$, it provides an accurate description at all r-values (figure 4(c)), which is consistent with the appearance of a sharp and dominant principal peak in $S_{CC}(k)$. An exponentially damped oscillatory function does not, however, provide a good description of $rh_{NC}(r)$ at large r. The wavelength of the oscillations for $rh_{NN}(r)$ and $rh_{CC}(r)$ is again given by $2\pi/a_1 \approx 2\pi/k_{PP}$, but, in accordance with the measured k_{PP} values, it is rather different for each of these functions (table 1). The oscillations in $rh_{CC}(r)$ also decay more slowly than those for $rh_{NN}(r)$. Within the framework of a simple ionic model, the observed behaviour for l-Ag_2Se could be rationalized in terms of an asymptotic regime that has not yet been reached in the measured $rh_{IJ}(r)$-functions; i.e., a common decay length and common wavelength of oscillation would be observed if data with sufficient accuracy were available at larger r-values. Alternatively, it may be necessary to move beyond a description of this system in terms of pair potentials as indicated by the need to use first principles molecular dynamics methods to accurately reproduce measured features such as the Ag–Ag pair distribution function [65, 83].

For liquid GeSe it proved difficult to satisfactorily fit the large-r behaviour of the $rh_{IJ}(r)$-functions by using an exponentially damped oscillatory function, and the fitted functions do not describe the $rh_{IJ}(r)$ over a wide r-range (figure 4(b)). For liquid CuSe, by comparison, an exponentially damped oscillatory function does provide a good account of the measured $rh_{NN}(r)$ and $rh_{NC}(r)$-functions over a large r-range, although the corresponding agreement with the measured $rh_{CC}(r)$-function is not as impressive (figure 4(a)). For l-CuSe, the fitted wavelength of the oscillations is given by $2\pi/a_1 \approx 2\pi/k_{PP}$ for $rh_{NN}(r)$ and $rh_{NC}(r)$ but not for $rh_{CC}(r)$ (table 1). In reciprocal space, $S_{NN}(k)$ shows the largest differences between the measured partial structure factors for liquid GeSe and CuSe (figures 1(a) and (b)). The liquid

phase of both these materials is characterized by a large number of homo-polar bonds [62–64]; i.e., the ability of an exponentially damped oscillatory function to account for the large-r behaviour in l-CuSe is unlikely to result from a predominantly ionic interaction model for this system. The reason for the differences between the structure of these liquid semiconductors merits further investigation; e.g., first-principles molecular dynamics simulations of liquid CuSe would complement those already made for liquid GeSe [84].

4.2. Limitations associated with the simple theory

We find that the large-r behaviour of the measured $rh_{IJ}(r)$-functions for a variety of systems, that include the network forming glasses $GeSe_2$, $ZnCl_2$ and GeO_2, can be adequately described in terms of exponentially damped oscillatory functions with a wavelength of oscillation given by $2\pi/a_1 \approx 2\pi/k_{PP}$, where k_{PP} is the position of the principal peak in the corresponding partial structure factor. In some cases, which include the measured $rh_{CC}(r)$ for the network glasses and l-Ag_2Se, an exponentially damped oscillatory function actually provides a good description of the measured data at most r-values. It also appears that the wavelength of this ordering at large r, which in network glasses is sometimes called the extended-range ordering since it extends to distances beyond the regime associated with the FSDP [10, 12], is sensitive to the repulsive part of the inter-atomic forces. For example, the observed periodicity $2\pi/a_1$ of 2.99(1), 2.96(1) and 2.34(1) Å for the network glasses $GeSe_2$, $ZnCl_2$ and GeO_2 (table 1) is comparable to the diameter of the larger (electronegative) species, namely 3.89(2), 3.70(1) and 2.83(1) Å respectively, where the latter values are taken from the position of the first main peak in the measured anion–anion partial pair distribution functions [10, 12, 69]. In binary mixtures of hard spheres having different diameters, the common wavelength of oscillation is set by one or other of these diameters depending on the thermodynamic state of the system [25].

An exponentially damped oscillatory decay of the $rh_{IJ}(r)$ functions is given by a pole analysis of the Ornstein–Zernike equations for model fluids with pair potentials that are of finite range [21, 23, 24] or for a rigid ion model of the pair potentials without dispersion terms [22]. In these models the principal pole is well separated from higher order poles and all of the poles are assumed to be simple. It is not obvious, however, that these simple pair potential models should apply to the systems for which experimental results are presented in section 3, since dispersion and three-body forces can be important. The presence of dispersion forces leads to an ultimate power law decay of the pair correlation functions as discussed in section 2.7. The presence of three- or higher-body interactions means that the potential energy of the system cannot be obtained by summing the pairwise additive potentials. In consequence, the large-r relation $c_{ij}(r) = -\beta\phi_{ij}(r)$ between the direct correlation function and the pair potential, which leads to equation (18) and the ensuing theoretical analysis, may need revision [49, 85]. It is however feasible that the analysis of section 2.5, which leads to an exponentially damped oscillatory decay of the $rh_{IJ}(r)$ functions with a common wavelength of oscillation and a common decay length, will hold provided $c_{ij}(r) = -\beta\phi_{ij}^{\text{eff}}(r)$, where $\phi_{ij}^{\text{eff}}(r)$ is an effective pair potential that leads to simple poles. Some evidence in support of this scenario is provided by the comparison between the experimental results for the network glasses and the predictions of simple theory shown in figures 5(b) and 6.

It would be interesting to make an analytical investigation of the poles obtained from the Ornstein–Zernike equations for model pair potentials in order to establish the extent to which a basic description of the extended-range ordering for a variety of systems such as molten salts [9], network glasses [12], amorphous metals [86] and colloids [87] can be provided by simple ideas such as charge ordering and packing constraints. For example, the principal peak remains a key feature in $S_{CC}(k)$ for network forming liquids and glasses, although chemical

ordering also occurs on the intermediate length scale as signified by the appearance of an FSDP (figures 2 and 3).

4.3. Requirement for experimental data over a wide k-range

To provide a more rigorous test of models for the forces of interaction in different systems, it would be advantageous to be able to accurately measure the partial structure factors over the widest possible range of k-values, including the small-k regime where the measured $S_{IJ}(k)$ are expected to be particularly sensitive to the details of the corresponding inter-atomic potentials (see e.g. sections 2.3 and 2.4). Indeed, small-angle scattering data have proved valuable for extracting information on two- and three-body potentials in rare gas fluids [88]. Diffraction data over a wide k-range would also prove useful for extracting effective inter-atomic potentials by the application of various inversion schemes [89, 90] and for providing more exacting constraints for use in structure refinement methods such as reverse Monte Carlo [91] and empirical potential structure refinement [92]. Progress in the field can be anticipated as new neutron diffraction instrumentation becomes available, such as the near- and intermediate-range order diffractometer (NIMROD) being constructed on the second target station at the ISIS pulsed neutron source [93], which will simultaneously measure the diffraction pattern for a sample at both small and large k-values.

5. Conclusion

We find that exponentially damped oscillatory decay of the pair correlation functions, as predicted from a simple theory with simple pair potentials, describes satisfactorily the measured data for the network glasses $GeSe_2$, $ZnCl_2$ and GeO_2. For each glass, a common decay length is observed for all of the measured $rh_{IJ}(r)$ and also a common wavelength for the oscillations, which is given by $\approx 2\pi/k_{PP}$, where k_{PP} is the position of the principal peak. However, the relations between the amplitudes predicted by the simple theory, namely $|\mathcal{A}_{NN}||\mathcal{A}_{CC}| = |\mathcal{A}_{NC}|^2$, does not appear to hold for any of the glasses and, although the relation between the phases $\theta_{NN} + \theta_{CC} = 2\theta_{NC}$ predicted by the simple theory does hold for glassy $ZnCl_2$ and $GeSe_2$, it does not appear to hold for glassy GeO_2. These discrepancies may arise from limitations associated with the measured data sets, from the effect of dispersion forces, or from the inability of pair potentials to accurately describe the system structure. For the liquid phase systems that were investigated, namely $GeSe_2$, Ag_2Se, GeSe and CuSe, the ability of an exponentially damped oscillatory function to account for the observed decay of the pair correlation functions meets with mixed success. For example, in the case of liquid Ag_2Se an exponentially damped oscillatory function accurately accounts for the measured $rh_{CC}(r)$ at all r-values but does not provide a good description of the measured $rh_{NC}(r)$ even at large r. For all of these liquids it is necessary to go beyond simple pair potentials in order to account for measured features such as the homopolar bonds which occur in $GeSe_2$, GeSe and CuSe. The subject would clearly benefit from more theoretical analysis of the systems studied experimentally and it is plausible that the asymptotic decay of the pair correlation functions, or equivalently the small-k behaviour of the measured structure factors, will provide a route for distinguishing between materials that are in some sense ionic (e.g. $ZnCl_2$) and those that are not (e.g. GeSe).

Acknowledgments

I am grateful to Bob Evans, Andrew Archer, Adrian Barnes, Paul Madden and Mark Wilson for many valuable discussions. Manon Lafouresse provided support during the development of this work.

Appendix A. The effect of ion-induced dipole interactions

Consider the case when the pair potentials of equation (17) are augmented to include a term $\propto r^{-4}$ which represents ion-induced dipole interactions

$$\phi_{ij}(r) = \phi_{ij}^{\rm sr}(r) + \frac{Z_i Z_j e^2}{\epsilon\, r} - \frac{P_{ij}}{r^4} - \frac{A_{ij}}{r^6} \tag{A.1}$$

where P_{ij} is a parameter ($\geqslant 0$) which depends on the polarizability of the ions and their charges [94, 95]. Following the procedure given in section 2.2, the Fourier transform of the large-r part of the direct correlation function is given by

$$\hat{c}_{ij}(k) = \hat{c}_{ij}^{\rm sr}(k) - \frac{4\pi\beta Z_i Z_j e^2}{\epsilon\, k^2} + p_{ij}\, k + \alpha_{ij}\, k^3 \tag{A.2}$$

where $p_{ij} = -\beta\pi^2 P_{ij}$ and the corresponding Bhatia–Thornton partial structure factors are given by

$$\begin{aligned}
S_{\rm NN}(k) &= \frac{\kappa_{\rm D}^2 + \left[1 - \rho\hat{c}_{\rm CC}^{\rm sr}(k)\right]k^2 - \rho p_{\rm CC}\, k^3 - \rho\alpha_{\rm CC}\, k^5}{k^2 D(k)}, \\
\frac{S_{\rm CC}(k)}{x_a x_b} &= \frac{\left[1 - \rho\hat{c}_{\rm NN}^{\rm sr}(k)\right]k^2 - \rho p_{\rm NN}\, k^3 - \rho\alpha_{\rm NN}\, k^5}{k^2 D(k)}, \\
\frac{S_{\rm NC}(k)}{x_a x_b} &= \frac{\rho\hat{c}_{\rm NC}^{\rm sr}(k)\, k^2 + \rho p_{\rm NC}\, k^3 + \rho\alpha_{\rm NC} k^5}{k^2 D(k)}.
\end{aligned} \tag{A.3}$$

In these equations $p_{\rm NN}$, $p_{\rm CC}$ and $p_{\rm NC}$ are defined in terms of the p_{ij} for the individual chemical species by expressions that are equivalent to equations (26)–(28) and the common denominator is given by

$$\begin{aligned}
k^2 D(k) = {} & \kappa_{\rm D}^2\left[1 - \rho\hat{c}_{\rm NN}^{\rm sr}(k)\right] - \rho p_{\rm NN}\kappa_{\rm D}^2\, k \\
& + \left[(1 - \rho\hat{c}_{\rm NN}^{\rm sr}(k))(1 - \rho\hat{c}_{\rm CC}^{\rm sr}(k)) - \rho_a\rho_b\, \hat{c}_{\rm NC}^{\rm sr}(k)^2\right]k^2 \\
& - \left[\rho\,\alpha_{\rm NN}\,\kappa_{\rm D}^2 + \rho p_{\rm NN}(1 - \rho\hat{c}_{\rm CC}^{\rm sr}) + \rho p_{\rm CC}(1 - \rho\hat{c}_{\rm NN}^{\rm sr}) - 2\rho_a\rho_b\hat{c}_{\rm NC}^{\rm sr} p_{\rm NC}\right]k^3 \\
& + \left[\rho^2 p_{\rm NN} p_{\rm CC} - \rho_a\rho_b p_{\rm NC}^2\right]k^4 \\
& - \left[\rho\alpha_{\rm NN}(1 - \rho\hat{c}_{\rm CC}^{\rm sr}(k)) + \rho\alpha_{\rm CC}(1 - \rho\hat{c}_{\rm NN}^{\rm sr}(k)) + 2\rho_a\rho_b\,\alpha_{\rm NC}\hat{c}_{\rm NC}^{\rm sr}(k)\right]k^5 \\
& + \left[\rho^2(p_{\rm NN}\alpha_{\rm CC} + p_{\rm CC}\alpha_{\rm NN}) - 2\rho_a\rho_b\, p_{\rm NC}\alpha_{\rm NC}\right]k^6 \\
& + \left[\rho^2\alpha_{\rm NN}\alpha_{\rm CC} - \rho_a\rho_b\,\alpha_{\rm NC}^2\right]k^8.
\end{aligned} \tag{A.4}$$

At small k it follows, by using the procedure given in section 2.3, that

$$S_{\rm NN}(k) = \frac{1}{(1 - \rho\hat{c}_{\rm NN}^{\rm sr(0)})} + \frac{p_{\rm NN}}{(1 - \rho\hat{c}_{\rm NN}^{\rm sr(0)})^2}\,\rho\, k + {\rm O}(k^2), \tag{A.5}$$

$$\begin{aligned}
\frac{S_{\rm CC}(k)}{x_a x_b} = {} & \frac{k^2}{\kappa_{\rm D}^2} - \frac{(1 - \rho\hat{c}_{\rm NN}^{\rm sr(0)})(1 - \rho\hat{c}_{\rm CC}^{\rm sr(0)}) - \rho_a\rho_b(\hat{c}_{\rm NC}^{\rm sr(0)})^2}{\kappa_{\rm D}^4(1 - \rho\hat{c}_{\rm NN}^{\rm sr(0)})}\,k^4 \\
& + \frac{\rho\rho_a\rho_b\, p_{\rm NN}(\hat{c}_{\rm NC}^{\rm sr(0)})^2 + \rho p_{\rm CC}(1 - \rho\hat{c}_{\rm NN}^{\rm sr(0)})^2 - 2\rho_a\rho_b\, p_{\rm NC}\hat{c}_{\rm NC}^{\rm sr(0)}(1 - \rho\hat{c}_{\rm NN}^{\rm sr(0)})}{\kappa_{\rm D}^4(1 - \rho\hat{c}_{\rm NN}^{\rm sr(0)})^2}\,k^5 \\
& + {\rm O}(k^6),
\end{aligned} \tag{A.6}$$

$$\frac{S_{\rm NC}(k)}{x_a x_b} = \frac{\rho\hat{c}_{\rm NC}^{\rm sr(0)}}{\kappa_{\rm D}^2(1 - \rho\hat{c}_{\rm NN}^{\rm sr(0)})}\,k^2 + \frac{\rho p_{\rm NC}(1 - \rho\hat{c}_{\rm NN}^{\rm sr(0)}) + \rho^2 p_{\rm NN}\hat{c}_{\rm NC}^{\rm sr(0)}}{\kappa_{\rm D}^2(1 - \rho\hat{c}_{\rm NN}^{\rm sr(0)})^2}\,k^3 + {\rm O}(k^4) \tag{A.7}$$

i.e. the term with the lowest odd integer power of k for $S_{\rm NN}(k)$, $S_{\rm NC}(k)$ and $S_{\rm CC}(k)$ is proportional to k, k^3 and k^5 respectively. The coefficients of the even powers of k smaller than the first odd power are the same as those given in equations (38)–(40). By using the procedure described in section 2.7 it follows that the ultimate large-r behaviour of the total pair correlation functions is given by $rh_{\rm NN}(r) \to -\mathcal{C}^{(1)}/\pi^2 r^3$, $rh_{\rm NC}(r) \to 12\mathcal{C}^{(3)}/\pi^2 r^5$ and $rh_{\rm CC}(r) \to -360\mathcal{C}^{(5)}/\pi^2 r^7$, where $\mathcal{C}^{(1)}$, $\mathcal{C}^{(3)}$ and $\mathcal{C}^{(5)}$ give the coefficients of the k, k^3 and k^5 terms in equations (A.5), (A.7) and (A.6) respectively. The small-k behaviour of the structure factor $S(k)$ and its derivatives for single-component classical fluids interacting with a pair potential of the form $\phi(r) \sim r^{-n}$ as $r \to \infty$, with n an integer > 3, is described by Nixon and Silbert [96].

Appendix B. The Lorch modification function

Let us consider a single-component liquid or glass. The Fourier transform expression which relates the structure factor $S(k)$ to the pair distribution function $g(r)$ for an isotropic system is given by

$$g(r) - 1 = \frac{1}{2\pi^2 \rho\, r} \int_0^\infty {\rm d}k\, k\, [S(k) - 1] \sin(kr) \tag{B.1}$$

where ρ is the atomic number density. This equation can be re-written as

$$-2\pi {\rm i} \rho\, r \left[g(r) - 1\right] = \frac{1}{2\pi} \int_{-\infty}^\infty {\rm d}k\, k\, [S(k) - 1] \exp(-{\rm i}kr) \tag{B.2}$$

where $S(k)$ has been extended to negative argument by defining it as an even function and ${\rm i} = \sqrt{-1}$. In a diffraction experiment, $S(k)$ will be truncated at some finite maximum value, $k_{\rm max}$, so the experiment will not give complete information about every point in r-space. For example, if a fast Fourier transform algorithm is employed, the range $0 \leqslant k \leqslant k_{\rm max}$ is divided into $\mathcal{N}$ mesh points of equal spacing, which gives rise to $\mathcal{N}$ mesh points in r-space of equal spacing $\pi/k_{\rm max}$ [97]. The average of $r[g(r) - 1]$ over an interval $\Delta = 2\pi/k_{\rm max}$ can be written as

$$\frac{-2\pi {\rm i} \rho}{\Delta} \int_{r-\Delta/2}^{r+\Delta/2} {\rm d}r\, r \left[g(r) - 1\right] = \frac{1}{\pi \Delta} \int_0^{k_{\rm max}} {\rm d}k\, k\, [S(k) - 1] \int_{r-\Delta/2}^{r+\Delta/2} {\rm d}r \exp(-{\rm i}kr) \tag{B.3}$$

and, provided Δ is sufficiently small, $r[g(r) - 1]$ will be approximately constant over the range from $r + \Delta/2$ to $r - \Delta/2$. By integrating with respect to r and then equating the imaginary parts in equation (B.3), it follows that

$$g(r) - 1 = \frac{1}{2\pi^2 \rho\, r} \int_0^{k_{\rm max}} {\rm d}k\, k\, [S(k) - 1]\ M(k) \sin(kr) \tag{B.4}$$

where $M(k) = \sin(ak)/(ak)$, with $a \equiv \Delta/2 = \pi/k_{\rm max}$, is called the Lorch modification function [70], which has a first zero at $k = k_{\rm max}$.

To find the peak-shape function in r-space that corresponds to the Lorch modification function $M(k)$, consider the Fourier transform pair

$$M(r) = \frac{1}{2\pi} \int_{-\infty}^\infty {\rm d}k\, M(k) \exp(-{\rm i}kr) \tag{B.5}$$

and

$$\mathcal{F}(r) = \frac{1}{2\pi} \int_{-\infty}^\infty {\rm d}k\, \mathcal{F}(k) \exp(-{\rm i}kr) \tag{B.6}$$

where $\mathcal{F}(k)$ is an even function given by $\mathcal{F}(k) = 1$ for $|k| \leqslant k_{\max}$ and $\mathcal{F}(k) = 0$ for $|k| > k_{\max}$. $M(r)$ is given by $M(r) = (2a)^{-1}$ for $|r| \leqslant a$ and by $M(r) = 0$ for $|r| > a$ but does not correspond to the required peak-shape function because $M(k) \neq 0$ for $k > k_{\max}$. Instead, the peak-shape function is given by the Fourier transform relation

$$P(r) = \frac{1}{2\pi} \int_{-\infty}^{\infty} \mathrm{d}k\, P(k) \exp(-\mathrm{i}kr) \tag{B.7}$$

where $P(k) \equiv \mathcal{F}(k)M(k)$ and $\mathcal{F}(r) = (\pi r)^{-1} \sin(\pi r/a)$. By the one-dimensional convolution theorem [98] it then follows that

$$\begin{aligned} P(r) &= \int_{-\infty}^{\infty} \mathcal{F}(r')M(r - r')\,\mathrm{d}r \\ &= \frac{1}{2\pi a} \int_{r-a}^{r+a} \frac{\sin(\pi r'/a)}{r'}\,\mathrm{d}r' \\ &= \frac{1}{2\pi a} \left[\mathrm{Si}\left(\frac{\pi(r+a)}{a}\right) - \mathrm{Si}\left(\frac{\pi(r-a)}{a}\right) \right] \end{aligned} \tag{B.8}$$

where the sine integral $\mathrm{Si}(x) \equiv \int_0^x \sin(t)/t\,\mathrm{d}t$. The maximum of the peak-shape function occurs at $P(0) = \mathrm{Si}(\pi)/(\pi a) = 0.1876\, k_{\max}$ and its full width at half maximum is given by $5.4366/k_{\max}$. Note that $P(k)$ is given by the inverse Fourier transform

$$P(k) = \int_{-\infty}^{\infty} \mathrm{d}r\, P(r) \exp(\mathrm{i}kr) \tag{B.9}$$

and the area under the peak-shape function is unity since

$$\int_{-\infty}^{\infty} \mathrm{d}r\, P(r) = P(k = 0) = 1. \tag{B.10}$$

Appendix C. Diffractometer with a Gaussian resolution function

For simplicity, consider the case of a diffractometer with a Gaussian resolution function [99]

$$\mathcal{P}(k) = \frac{\exp\{-k^2/2(\Delta k)^2\}}{(2\pi)^{1/2}\Delta k} \tag{C.1}$$

where Δk is the standard deviation and, since the resolution function does not create or annihilate intensity but simply redistributes the available intensity across the measured diffraction pattern, the area of the Gaussian is chosen to be unity. The Fourier transform of $\mathcal{P}(k)$ is given by

$$\mathcal{P}(r) = \frac{1}{2\pi} \int_{-\infty}^{\infty} \mathrm{d}k\, \mathcal{P}(k) \exp(-\mathrm{i}kr) = \frac{1}{2\pi} \exp\{-(\Delta k)^2 r^2/2\} \tag{C.2}$$

and, as shown in equation (B.2), the Fourier transform of $-2\pi\mathrm{i}\rho\, r h(r)$ is given by $k\,[S(k) - 1]$, where $h(r) \equiv [g(r) - 1]$. By the one-dimensional convolution theorem [98] it then follows that

$$\frac{1}{2\pi} \int_{-\infty}^{\infty} \mathrm{d}k\, \{k\,[S(k) - 1] \otimes \mathcal{P}(k)\} \exp(-\mathrm{i}kr) = 2\pi\{-2\pi\mathrm{i}\rho\, r h(r)\mathcal{P}(r)\} \tag{C.3}$$

where $\otimes$ denotes the one-dimensional convolution operator. Hence, by equating the imaginary parts in equation (C.3), it can be readily shown that

$$\begin{aligned} h'(r) &\equiv \frac{1}{2\pi^2 \rho\, r} \int_0^{\infty} \mathrm{d}k\, \{k\,[S(k) - 1] \otimes \mathcal{P}(k)\} \sin(kr) \\ &= 2\pi h(r)\mathcal{P}(r) \\ &= h(r) \exp\{-(\Delta k)^2 r^2/2\} \end{aligned} \tag{C.4}$$

i.e. the effect of a diffractometer with a Gaussian resolution function of constant width is to damp exponentially the total pair correlation function.

References

[1] Moss S C and Price D L 1985 *Physics of Disordered Materials* ed D Adler, H Fritzsche and S R Ovshinsky (New York: Plenum) p 77
[2] Elliott S R 1991 *Nature* **354** 445
[3] Salmon P S 1994 *Proc. R. Soc.* A **445** 351
[4] Elliott S R 1995 *J. Non-Cryst. Solids* **182** 40
[5] Gaskell P H and Wallis D J 1996 *Phys. Rev. Lett.* **76** 66
[6] Salmon P S 2002 *Nat. Mater.* **1** 87
[7] Massobrio C, Celino M and Pasquarello A 2004 *Phys. Rev.* B **70** 174202
[8] Sharma B K and Wilson M 2006 *Phys. Rev.* B **73** 060201
[9] Salmon P S 1992 *Proc. R. Soc.* A **437** 591
[10] Salmon P S, Martin R A, Mason P E and Cuello G J 2005 *Nature* **435** 75
[11] Salmon P S 2005 *J. Phys.: Condens. Matter* **17** S3537
[12] Salmon P S, Barnes A C, Martin R A and Cuello G J 2006 *Phys. Rev. Lett.* **96** 235502
[13] Angell C A 1995 *Science* **267** 1924
[14] Angell C A 1985 *J. Non-Cryst. Solids* **73** 1
[15] Polsky C H, Martinez L M, Leinenweber K, VerHelst M A, Angell C A and Wolf G H 2000 *Phys. Rev.* B **61** 5934
[16] Wilson M 2003 *J. Chem. Phys.* **118** 9838
[17] Poole P H, Grande T, Angell C A and McMillan P F 1997 *Science* **275** 322
[18] McMillan P F 2004 *J. Mater. Chem.* **14** 1506
[19] Gibson H M and Wilding N B 2006 *Phys. Rev.* E **73** 061507
Gibson H M and Wilding N B 2006 *Phys. Rev.* E **74** 019903
[20] Wilding M C, Wilson M and McMillan P F 2006 *Chem. Soc. Rev.* **35** 964
[21] Evans R, Leote de Carvalho R J F, Henderson J R and Hoyle D C 1994 *J. Chem. Phys.* **100** 591
[22] Leote de Carvalho R J F and Evans R 1994 *Mol. Phys.* **83** 619
[23] Leote de Carvalho R J F, Evans R, Hoyle D C and Henderson J R 1994 *J. Phys.: Condens. Matter* **6** 9275
[24] Dijkstra M and Evans R 2000 *J. Chem. Phys.* **112** 1449
[25] Grodon C, Dijkstra M, Evans R and Roth R 2004 *J. Chem. Phys.* **121** 7869
[26] Grodon C, Dijkstra M, Evans R and Roth R 2005 *Mol. Phys.* **103** 3009
[27] Rino J P, Ebbsjö I, Branicio P S, Kalia R K, Nakano A, Shimojo F and Vashishta P 2004 *Phys. Rev.* B **70** 045207
[28] Donev A, Stillinger F H and Torquato S 2005 *Phys. Rev. Lett.* **95** 090604
[29] Pearson F J and Rushbrooke G S 1957 *Proc. R. Soc. Edinburgh* A **64** 305
[30] Hansen J P and McDonald I R 2006 *Theory of Simple Liquids* 3rd edn (Amsterdam: Academic)
[31] McQuarrie D A 2000 *Statistical Mechanics* (Sausalito, CA: University Science Books)
[32] Bhatia A B and Thornton D E 1970 *Phys. Rev.* B **2** 3004
[33] Cusack N E 1987 *The Physics of Structurally Disordered Matter* (Bristol: Hilger) chapter 10
[34] Rovere M, Parrinello M, Tosi M P and Giaquinta P V 1979 *Phil. Mag.* B **39** 167
[35] Kjellander R and Forsberg B 2005 *J. Phys. A: Math. Gen.* **38** 5405
[36] Enderby J E, Gaskell T and March N H 1965 *Proc. Phys. Soc.* **85** 217
[37] Torquato S and Stillinger F H 2003 *Phys. Rev.* E **68** 041113
[38] Faber T E and Ziman J M 1965 *Phil. Mag.* **11** 153
[39] Fournet G 1957 *Handbuch der Physik* vol 32 (Berlin: Springer) p 238
[40] Fischer H E, Barnes A C and Salmon P S 2006 *Rep. Prog. Phys.* **69** 233
[41] Chieux P and Ruppersberg H 1980 *J. Physique Coll.* **C8** 145
[42] Pyper N C 1991 *Adv. Solid State Chem.* vol 2, ed C R A Catlow (London: JAI Press) p 223
[43] Sangster M J L and Dixon M 1976 *Adv. Phys.* **25** 247
[44] Wilson M and Madden P A 1993 *J. Phys.: Condens. Matter* **5** 6833
[45] Hutchinson F, Rowley A J, Walters M K, Wilson M, Madden P A, Wasse J C and Salmon P S 1999 *J. Chem. Phys.* **111** 2028
[46] Rovere M and Tosi M P 1986 *Rep. Prog. Phys.* **49** 1001
[47] Stillinger F H Jr and Lovett R 1968 *J. Chem. Phys.* **49** 1991
[48] Casimir H B G and Polder D 1948 *Phys. Rev.* **73** 360
[49] Reatto L and Tau M 1992 *J. Phys.: Condens. Matter* **4** 1

[50] Fisher M E and Widom B 1969 *J. Chem. Phys.* **50** 3756
[51] Hopkins P, Archer A J and Evans R 2005 *Phys. Rev.* E **71** 027401
[52] Hopkins P, Archer A J and Evans R 2006 *J. Chem. Phys.* **124** 054503
[53] Evans R and Sluckin T J 1981 *J. Phys. C: Solid State Phys.* **14** 2569
[54] Salmon P S and Liu J 1994 *J. Phys.: Condens. Matter* **6** 1449
[55] Stillinger F H Jr and Lovett R 1968 *J. Chem. Phys.* **48** 3858
[56] Lighthill M J 1958 *Introduction to Fourier Analysis and Generalised Functions* (Cambridge: Cambridge University Press) p 56
[57] Maret M, Chieux P, Dubois J M and Pasturel A 1991 *J. Phys.: Condens. Matter* **3** 2801
[58] Westlake J R 1968 *A Handbook of Numerical Matrix Inversion and Solution of Linear Equations* (New York: Wiley)
[59] Biggin S and Enderby J E 1982 *J. Phys. C: Solid State Phys.* **15** L305
[60] Biggin S and Enderby J E 1981 *J. Phys. C: Solid State Phys.* **14** 3577
[61] McGreevy R L and Mitchell E W J 1982 *J. Phys. C: Solid State Phys.* **15** 5537
[62] Barnes A C and Enderby J E 1988 *Phil. Mag.* B **58** 497
[63] Petri I, Salmon P S and Fischer H E 1999 *J. Phys.: Condens. Matter* **11** 7051
[64] Petri I, Salmon P S and Fischer H E 1999 *J. Non-Cryst. Solids* **250–252** 405
[65] Barnes A C, Lague S B, Salmon P S and Fischer H E 1997 *J. Phys.: Condens. Matter* **9** 6159
[66] Penfold I T and Salmon P S 1990 *J. Phys.: Condens. Matter* **2** SA233
[67] Penfold I T and Salmon P S 1991 *Phys. Rev. Lett.* **67** 97
[68] Petri I, Salmon P S and Fischer H E 2000 *Phys. Rev. Lett.* **84** 2413
[69] Salmon P S and Petri I 2003 *J. Phys.: Condens. Matter* **15** S1509
[70] Lorch E 1969 *J. Phys. C: Solid State Phys.* **2** 229
[71] Salmon P S, Petri I, de Jong P H K, Verkerk P, Fischer H E and Howells W S 2004 *J. Phys.: Condens. Matter* **16** 195
[72] Blank H and Maier H (ed) 1988 *Guide to Neutron Research Facilities* (Grenoble: Institut Laue-Langevin) p 20
[73] Fischer H E, Cuello G J, Palleau P, Feltin D, Barnes A C, Badyal Y S and Simonson J M 2002 *Appl. Phys.* A **74** S160
[74] Wright A C, Sinclair R N and Leadbetter A J 1985 *J. Non-Cryst. Solids* **71** 295
[75] Wilson M, Madden P A, Hemmati M and Angell C A 1996 *Phys. Rev. Lett.* **77** 4023
[76] Gray-Weale A and Madden P A 2003 *Mol. Phys.* **101** 1761
[77] Cobb M, Drabold D A and Cappelletti R L 1996 *Phys. Rev.* B **54** 12162
[78] Cobb M and Drabold D A 1997 *Phys. Rev.* B **56** 3054
[79] Massobrio C, Pasquarello A and Car R 2001 *Phys. Rev.* B **64** 144205
[80] Massobrio C and Pasquarello A 2003 *Phys. Rev.* B **68** 020201
[81] Mei Q, Benmore C J, Hart R T, Bychkov E, Salmon P S, Martin C D, Michel F M, Antao S M, Chupas P J, Lee P L, Shastri S D, Parise J B, Leinenweber K, Amin S and Yarger J L 2006 *Phys. Rev.* B **74** 014203
[82] Guthrie M, Tulk C A, Benmore C J, Xu J, Yarger J L, Klug D D, Tse J S, Mao H-k and Hemley R J 2004 *Phys. Rev. Lett.* **93** 115502
[83] Kirchhoff F, Holender J M and Gillan M J 1996 *Phys. Rev.* B **54** 190
[84] van Roon F H M, Massobrio C, de Wolff E and De Leeuw S W 2000 *J. Chem. Phys.* **113** 5425
[85] Reatto L and Tau M 1987 *J. Chem. Phys.* **86** 6474
[86] Miracle D B 2004 *Nat. Mater.* **3** 697
[87] Campbell A I, Anderson V J, van Duijneveldt J S and Bartlett P 2005 *Phys. Rev. Lett.* **94** 208301
[88] Formisano F, Benmore C J, Bafile U, Barocchi F, Egelstaff P A, Magli R and Verkerk P 1997 *Phys. Rev. Lett.* **79** 221
[89] Dharma-wardana M W C and Aers G C 1983 *Phys. Rev.* B **28** 1701
[90] Levesque D, Weis J J and Reatto L 1985 *Phys. Rev. Lett.* **54** 451
[91] McGreevy R L 2001 *J. Phys.: Condens. Matter* **13** R877
[92] Soper A K 2005 *Phys. Rev.* B **72** 104204
[93] Taylor A 2000 *Physica* B **276–278** 36 and http://www.isis.rl.ac.uk/targetstation2/scienceCase/
[94] Vashishta P and Rahman A 1978 *Phys. Rev. Lett.* **40** 1337
[95] Bitrián V and Trullàs J 2006 *J. Phys. Chem.* B **110** 7490
[96] Nixon J H and Silbert M 1982 *J. Phys. C: Solid State Phys.* **15** L165
[97] Lado F 1971 *J. Comput. Phys.* **8** 417
[98] Champeney D C 1973 *Fourier Transforms and their Physical Applications* (London: Academic)
[99] Grimley D I, Wright A C and Sinclair R N 1990 *J. Non-Cryst. Solids* **119** 49